https://doi.org/10.5194/bg-2020-314
Preprint. Discussion started: 4 September 2020

Biogeosciences Discussions

Modelling Silicate – Nitrate - Ammonium co-limitation of algal growth and the importance of bacterial remineralisation based on an experimental Arctic coastal spring bloom culture study

Tobias R. Vonnahme[1], Martial Leroy[2], Silke Thoms[3], Dick van Oevelen[4], H. Rodger Harvey[5], Svein Kristiansen[1], Rolf Gradinger[1], Ulrike Dietrich[1], Christoph Voelker[3]

[1] Department of Arctic and Marine Biology, UiT – The Arctic University of Norway, Tromsø, Norway
[2] Université Grenoble Alpes, Grenoble, France
[3] Alfred-Wegener Institute for Polar and Marine Research, Bremerhaven, Germany
[4] Department of Estuarine and Delta Systems, NIOZ Royal Netherlands Institute for Sea Research, and Utrecht University, Texel, Yerseke, Netherlands
[5] Department of Ocean and Earth Sciences, Old Dominion University, Norfolk, USA

Correspondence to: Tobias R. Vonnahme (Tobias.Vonnahme@uit.no) and Christoph Voelker (christoph.voelker@awi.de)

Abstract. Arctic coastal ecosystems are rapidly changing due to climate warming, which makes modelling their productivity crucially important to better understand future changes. System primary production in these systems is highest during the pronounced spring bloom, typically dominated by diatoms. Eventually the spring blooms terminate due to silicon or nitrogen limitation. Bacteria can play an important role for extending bloom duration and total CO_2 fixation through ammonium regeneration. Current ecosystem models often simplify the effects of nutrient co-limitations on algal physiology and cellular ratios and neglect bacterial driven regeneration, leading to an underestimation of primary production. Detailed biochemistry- and cell-based models can represent these dynamics but are difficult to tune in the environment. We performed a cultivation experiment that showed typical spring bloom dynamics, such as extended algal growth via bacteria ammonium remineralisation, and reduced algal growth and inhibited chlorophyll synthesis under silicate limitation, and gradually reduced nitrogen assimilation and chlorophyll synthesis under nitrogen limitation. We developed a simplified dynamic model to represent these processes. The model also highlights the importance of organic matter excretion, and post bloom ammonium accumulation. Overall, model complexity is comparable to other ecosystem models used in the Arctic while improving the representation of nutrient co-limitation related processes. Such model enhancements that now incorporate increased nutrient inputs and higher mineralization rates in a warmer climate will improve future predictions in this vulnerable system.

https://doi.org/10.5194/bg-2020-314
Preprint. Discussion started: 4 September 2020

1 Introduction

Marine phytoplankton is responsible for half of the CO_2 fixation on Earth (Field et al., 1998; Westberry et al., 2008). Diatoms in high latitude oceans are an important group contributing 20-40% of the global CO_2 fixation (Nelson et al., 1995; Uitz et al., 2010). Marine primary production can be bottom-up limited by light or nutrients like nitrogen (N), phosphorous (P), silicon (Si), and iron (Fe) with pronounced geographical and seasonal variations in their availability (Eilertsen et al., 1989; Loebl et al., 2009; Iversen and Seuthe, 2011; Moore et al., 2013). Arctic coasts are one of the fastest changing systems due to climate change and modelling their dynamics is difficult but crucial for predictions (e.g. Slagstad et al., 2015; Fritz et al., 2017). In Arctic coastal ecosystems primary production is typically highest in spring, after winter mixing supplied fresh nutrients, sea ice has melted, and combined with increasing temperatures, caused the formation of a stratified surface layer with sufficient light (Sverdrup, 1953; Eilertsen et al., 1989; Eilertsen and Frantzen, 2007; Iversen and Seuthe, 2011). With increasing temperatures and runoff, stratification in coastal Arctic systems is expected to increase, leading to decreased mixing and nutrient upwelling in autumn and winter and an earlier stratified surface layer in spring (Tremblay and Gagnon, 2009). The spring bloom typically consists of chain-forming diatoms and is terminated by Si or N limitation (Eilertsen et al., 1989; Iversen and Seuthe, 2011). Bacteria remineralisation may supply additional N and Si (Legendre and Rassoulzadegan, 1995; Bidle and Azam, 1999; Johnson et al., 2007). However, N regeneration has been described as a mostly bacteria-related process (Legendre and Rassoulzadegan, 1995), while Si dissolution is mainly controlled by abiotic dissolution of silica (Bidle and Azam, 1999). A warmer climate will increase both bacteria-related remineralisation rates (Legendre and Rassoulzadegan, 1995) and abiotic silica dissolution (Bidle and Azam, 1999), but the magnitude is not well understood.

Phytoplankton blooms may be dominated by a single or a few algal species, often with a similar physiology during certain phases of the bloom (e.g. Eilertsen et al., 1989; Degerlund and Eilertsen, 2010; Iversen and Seuthe, 2011). In some Arctic and sub-Arctic areas the Arctic phytoplankton chosen for this model, *Chaetoceros socialis*, is a dominant species during spring blooms (Eilertsen et al., 1989; Booth et al., 2002; Degerlund and Eilertsen, 2010). Such spring phytoplankton blooms are accompanied by bacterioplankton blooms also showing typical succession patterns and distinct re-occurring taxa that dominate the community (Teeling et al., 2012; Teeling et al., 2016). The importance of bacterial nutrient recycling for regenerated production has been recognized in several ecosystem models (e.g. van der Meersche et al., 2004; Vichi et al., 2007; Weitz et al., 2015) and algae bioreactor models focussing on nutrient conversions (e.g. Zambrano et al., 2016), but is typically neglected in more sophisticated dynamic multi-nutrient, quota based models. These latter models have been often developed and tuned based on cultivation experiments in which microbial remineralization reactions were absent (e.g. Geider et al., 1998; Flynn, 2001) despite the fact that most algae cultures are not axenic and models based on these experiments ignore bacterial contributions to nutrient recycling. Additional positive effects of bacteria include vitamin synthesis (Amin et al., 2012), trace metal chelation (Amin et al., 2012), the scavenging of oxidative stressors (Hünken et al., 2008), and exchange of growth factors (Amin et al., 2015). However, especially in the stationary algal growth phase, Christie-Oleza et al. (2017) found that marine cyanobacteria cultures are dependent on bacteria contaminants mainly due to their importance in degrading potentially toxic

https://doi.org/10.5194/bg-2020-314
Preprint. Discussion started: 4 September 2020


Biogeosciences Discussions Open Access EGU

DOM exudates and regenerating ammonium. The current study aimed to bridge the gap between detailed representations of algae physiology and the role of microbial activity in an accurate way while keeping model complexity low.

Most ecosystem models consider only a single limiting nutrient to control primary production after Liebig's Law of the minimum (Wassmann et al., 2006; Vichi et al., 2007). Yet we know that nutrient co-limitation is more complex; i.e. ammonium can inhibit nitrate uptake (Flynn et al., 1997), iron has a strong control on silicate uptake (Werner, 1977; Hohn et al., 2009), and the effects on photosynthesis differs between nitrogen and silicon limitations (Werner, 1977; Flynn, 2003; Hohn et al., 2009). Complex interaction models considering intracellular biochemistry (NH_4-NO_3 co-limitation, Flynn et al., 1997) and cell cycles (Si limitation, Flynn, 2001) can accurately describe these dynamics (Flynn, 2003), but are ultimately too complex to be integrated and parameterized in large scale ecosystem models. Some models (Hohn et al., 2009, Le Quéré et al., 2016) implemented multinutrient (Hohn et al., 2009) and bacterial dynamics (Le Quéré et al., 2016) in Southern Ocean ecosystem models, but have their limitations in representing bacterial remineralisation (Hohn et al., 2009), or ammonium and silicate co-limitations (Le Quéré et al., 2016). In contrast to Antarctica, iron and phosphate are not limiting in most Arctic coastal systems. Controlled lab experiments, representing the major dynamics found in the environment and predicted with climate change, are needed to facilitate the development of simple, but accurate multinutrient models scalable to larger ecosystem models.

The current study investigated the relevance of silicate, ammonium - nitrate co-limitation, bacterial nutrient regeneration and changes in photosynthesis, nitrogen assimilation, and cellular quotas in response to the changing nutrient limitations based on data from a culture based Arctic spring bloom system. The culture consisted of an axenic isolate of *Chaetoceros socialis*, dominating a phytoplankton net haul of a Svalbard fjord, used experimentally either under axenic conditions or after inoculation with its associated bacteria. Parametrization and insights from these incubations were then used to develop and parameterize a simple Carbon quota based dynamic model (based on Geider et al., 1998), aiming to keep complexity low to allow its use in larger ecosystem models.

The aims of the study was I) to study the bloom dynamics of simplified Arctic coastal pelagic system in a culture experiment consisting of one Arctic diatom species and associated bacteria, II) to develop a simple dynamic model representing the observed cell interactions, and III) to discuss the importance of more complex bloom dynamics and their importance for an accurate ecosystem model.

We hypothesize that: I) Bacterial regeneration of ammonium will extend a phytoplankton growth period and gross carbon fixation; II) Silicate or nitrogen limitations will have different physiological effects and physiological responses; III) A simple growth experiment and dynamic model with three nutrient pools and bacterial DON regeneration can adequately represent Arctic spring bloom dynamics.

https://doi.org/10.5194/bg-2020-314
Preprint. Discussion started: 4 September 2020


Biogeosciences Discussions

2 Methods

2.1 Cultivation experiment

The most abundant phytoplankton species from a net haul (20µm mesh size) in April 2017 in van Mijenfjorden (Svalbard) *Chaetoceros socialis* was isolated via the dilution isolation method (Andersen et al., 2005) on F/2 medium (Guillard, 1975). Bacteria were isolated on LB-medium (evaluated by Bertani, 2004) Agar plates using the algae culture as inoculum and sequenced at GENEWIZ LLC using the Sanger method and standard 16S rRNA primers targeting the V1-V9 region (Forwards 5'- AGAGTTTGATCCTGGCTCAG -3', Reverse 5'- ACGGCTACCTTGTTACGACTT -3') provided by GENEWIZ LLC for identification via blastn (Altschul et al., 1990). Two strains of *Pseudoalteromonas elyakovii*, a taxon previously isolated from the Arctic (Khudary et al., 2008) and known to degrade algae polysaccharides (Ma et al., 2008) and to excrete polymeric substances (Kim et al., 2016), were successfully isolated and used for the experiments. Before the start of the experiment, all bacteria in the algae culture were killed using a mixture of the antibiotics penicillin and streptomycin. The success was confirmed via incubation of the cultures on LB-Agar plates and bacterial counts after DAPI staining (Porter et al., 1980). The axenic cultures were diluted in fresh F/2 medium lacking nitrate addition (Guillard, 1975) using sterile filtered seawater of Tromsø sound (Norway) as basis. The algae cultures were transferred into 96 200ml sterile cultivation bottles with three replicates for each treatment. Half of the incubations were inoculated with bacteria cultures, while the other half was kept axenic. The cultures were incubated at 4°C and 100 µE m^{-2} s^{-1} continuous light. Over 16 days three axenic and three bacteria-enriched bottles were sacrificed daily for measurements of chlorophyll a (Chl), particulate organic carbon (POC) and nitrogen (PON), bacteria cell numbers, algae cell numbers, nutrients (nitrate, nitrite, ammonium, phosphate, silicate), dissolved organic carbon (DOC), and the maximum quantum yield (QY) of PSII (Fv/Fm) as a measure of healthy photosystems.

Chlorophyll a was extracted from a GF/F (50ml filtered at 200mbar) filter at 4C° for 12-24h in 98% methanol in the dark before measurement in a Turner Trilogy™ Fluorometer (evaluated by Jacobsen and Rai, 1990). POC and PON were measured after filtration onto precombusted (4h at 450°C) GF/F (Whatman) filters (50ml filtered at 200mbar), using a Flash 2000 elemental analyser (Thermo Fisher Scientific, Waltham, MA, USA) and Euro elemental analyser (Hekatech) following the protocol by Pella and Colombo (1973) after removing inorganic carbon by fuming with saturated HCl in a desiccator. Bacteria were counted after fixation of a water sample for 3-4h with 2% Formaldehyde (final concentration), filtration of 25ml on 0.2µm pore size Polycarbonate filter, washing with filtered Seawater and Ethanol, DAPI staining for 7 minutes after Porter et al. (1980), and embedding in Citifluor-Vectashield (3:1). Bacteria were counted in at least 20 grids under an epifluorescence microscope (Leica DM LB2, Leica Microsystems, Germany) at 10x100 magnification. In the same sample the average diameter of diatom cells at the start and end of the experiment was measured. Algae were counted in 2ml wells under an inverted microscope (Zeiss Primovert, Carl Zeiss AG, Germany) at 20x10 magnification after gentle mixing of the cultivation bottle. Algae cells incorporated in biofilms after day 9 in the bacteria enriched cultures were counted after sonication in a sonication bath until all cells were in suspension. Nutrient and DOC samples were sterile filtered (0.2µm) and stored at -20°C before measurements. Nutrients were measured in triplicates after using standard colorimetric on a nutrient analyser (QuAAtro

https://doi.org/10.5194/bg-2020-314
Preprint. Discussion started: 4 September 2020

39, SEAL Analytical, Germany) using the protocols No. Q-068-05 Rev. 12 for nitrate (detection limit = 0.02 µmol L^{-1}), No. Q-068-05 Rev. 12 for nitrite (detection limit = 0.02 µmol L^{-1}), No. Q-066-05 Rev. 5 for silicate (detection limit = 0.07 µmol L^{-1}), and No. Q-064-05 Rev. 8 for phosphate (detection limit = 0.01 µmol L^{-1}). The data were analysed using the software AACE. The nutrient analyzer was calibrated with reference seawater (Ocean Scientific International Ltd., United Kingdom). Ammonium was measured manually using the colorimetric method after McCarthy et al., (1977) on a spectrophotometer (Shimadzu UV-1201, detection limit = 0.01 µmol L^{-1}). DOC was measured by high temperature catalytic oxidation (HTCO) using a Shimadzu TOC-5000 total C analyser following methods for seawater samples (Burdige and Homstead, 1994). The photosynthetic quantum yield was determined using an Aquapen PA-C 100 (Photon Systems Instruments, Czech Republic).

Certain factors, such as grazing, settling out of the euphotic zone, and bacterial and algae succession were not included into the experimental set-up to reduce complexity, and focus on nutrient dynamics. Trace metals, phosphate, and Vitamin B12 in coastal systems are assumed to be not limiting in Arctic coastal systems and were supplied in excess to the culture medium. Realistic pre-bloom DOC concentrations were present in the medium as it was prepared with sterilized seawater from the Fjord outside Tromsø before the onset of the spring bloom (March 2018).

All plots were done in R. The f-ratio as indication for the importance of regenerated production was calculated based on the average PON fixation in the last three days of the experiment. Here, nitrogen assimilation in the axenic culture was assumed to be based on new (nitrate based) production, while fixation in the bacteria-enriched experiment was assumed to also be based on regenerated (ammonium based) production.

2.2 Modelling

This section outlines briefly the overall model structure followed by a short description of the chosen parametrization approach for each relevant process. Details regarding model equations are provided in the Appendix (Table A1).

The Geider et al. (1998) model (G98) was used as a simple cell quota model to describe the response of phytoplankton to different nitrogen conditions. The G98 model is based on both intracellular quotas and extracellular nutrient concentrations, allowing decoupled C and N growth. It has been used in a variety of large scale ecosystem models with some extensions representing the actual conditions in the environment or mesocosms (e.g. Moore et al., 2004; Schartau et al., 2007; Hauck et al., 2013).

Photoacclimation dynamics in Geider type models have been evaluated as quick and robust (Flynn et al., 2001), while the N-assimilation component has some shortcomings in regard to ammonium-nitrate interactions. The original model of Geider et al. (1998) for C and N was corrected for minor typographical errors (see Ross and Geider, (2009), Appendix Tables A6 A7) and afterwards extended to represent dynamics and interactions of silicate, nitrate and ammonium uptake, carbon and nitrogen excretion and bacterial remineralisation. The aim of the study was to develop a model with simplified dynamics of nutrient co-limitation, which is suitable for future implementation in coupled biogeochemistry-circulation models. The aim of the model was to describe the response in photosynthesis, chlorophyll synthesis and nitrogen assimilation with a minimal number

https://doi.org/10.5194/bg-2020-314
Preprint. Discussion started: 4 September 2020

of parameters. Hence, dynamics in silicate cycling and bacterial physiology were highly simplified. The limitations of these simplifications and the potential need for more complex models are discussed later.

Silicate uptake was modelled using Monod kinetics after Spilling et al. (2010). The response of silicate limitation on photosynthesis and chlorophyll synthesis was implemented after Werner (1978), Martin-Jézéquel et al. (2000), and Claquin et al. (2002). Werner (1978) found that silicate limitation can lead to a 80% reduction in photosynthesis and a stop of chlorophyll synthesis in diatoms within a few hours. Nitrogen metabolism is typically not affected by silicate limitation (Hildebrand 2002, Claquin et al., 2002), but the growth rate can be reduced (Hildebrand, 2002; Gilpin, 2004).

The algal respiration term included both respiration and excretion of dissolved organic nitrogen and carbon as a fraction of the carbon and nitrogen assimilated. Dissolved organic nitrogen (DON) was recycled into ammonium via bacterial remineralisation. It was assumed that this process is faster for freshly excreted DON compared to DON already present in the medium. We also assumed that excreted DON and DOC do not coagulate as EPS during the course of the experiment. After Tezuka (1989), bacterial remineralisation occurs at substrate C/N mass ratio below 10 and is proportional to bacterial abundances. Higher thresholds up to 29 have been found (e.g. Kirchmann, 2000), but we selected a lower number to stay conservative. Substrate C/N ratios are assumed to be proportional to algae C/N ratios (van der Meersche et al., 2004), with algal C/N ratios below 10 representing substrate (DOM) C/N ratios below 10.5. Hence, we assume bacterial remineralisation to occur at POC/PON ratios below 10. Bacteria abundance change was estimated using a simple logistic growth curve as a function of DOM since the number of parameters is low (2) and the fit sufficient for the purpose of modelling algae physiology.

Algal nitrate uptake was modelled after the original model by Geider et al. (1998) and ammonium assimilation was based on the simplified SHANIM model by Flynn and Fasham (1997b), excluding the internal nutrient and glutamine concentrations. Ammonium uptake is preferred over nitrate (lower half saturation constant) and reduces nitrate assimilation if available above a certain threshold concentration of ammonium (Dortch, 1990; Flynn, 1999). Ammonium is the primary product of bacterial regeneration N-compound after remineralization of DON. Nitrification was assumed to be absent, since the bacteria in our experiment are not known to be capable of nitrification.

The model was written in R and all model equations are provided in the Appendix (Table A6). The differential equations were solved using the ode function of the deSolve package (Soetart et al., 2010) with the Runge-Kutte method. After sensitivity analyses using the sensFun function of the FME package (Soetart and Petzoldt, 2010) (Fig. B1), and collinearity tests using the collin function and pairs plots (Fig. B2) the parameters not available from the experimental data (14 for our model, 6 for G98) were fitted based on the data of both the axenic experiment (i.e. without remineralisation) and the bacteria enriched experiment (i.e. with remineralisation). The aim was to reach an optimal fit for both the axenic and bacteria enriched experiment using the same values for the parameters

The first parameter fitting was done using the traditional G98 model. The parameters maximum gChl:gN ratio (θ^{N}_{max}), minimum and maximum gN:gC ratios (Q_{min}, Q_{max}), and irradiance (I) were given by the experimental data and needed no further tuning. The start values for the remaining six variables were based on model fits of G98 to other diatom cultures in previous studies (Geider 1998, Ross and Geider 2009). Maximum C specific photosynthesis (P^{C}_{ref}) and C based maintenance

https://doi.org/10.5194/bg-2020-314
Preprint. Discussion started: 4 September 2020

metabolic rate (R^C) were collinear and only P^C_{ref} was fitted. Manual parameter fitting was done using constraints given by earlier studies (Geider et al., 1998; Ross and Geider, 2009). The model was fitted manually to reach an optimal fit for both the axenic and bacteria enriched experiment using the same values for the parameters, (Fig. 3,4), considering known limitations in the lag and stationary phase. The modFit function, using the Pseudorandom search algorithm, was based on the modCost function of the FME package and used to test whether potential substantial improvements of the model fit using different parameter values could be achieved, but this was not the case so manual fits were retained. The G98 model based parameters were kept for the tuning of the additional parameters of the extended model aiming to use the same parameter values for both experiments. Bacterial growth parameters (μ_{bact}, $bact_{max}$) were determined in the growth experiment. Silicate related parameters (K_{si}, V_{max}, s_{min}) were constrained by the study of Werner (1978). Ammonium related parameters (K_{nh4}, $nh4_{thres}$) were constrained loosely by measured ammonium concentrations, and remineralisation parameters (rem, rem_d) were left unconstrained. Collinearity tests, and manual and automated parameter fitting were done as described for the G98 model. Eventually, the 14 parameters (Table A3) were fitted against 160 data points (Table A1). The model cost was estimated via calculating the root of the sum of squares normalized by dividing the squares with the variance (RMSE Eq. (C1), Stow et al., 2009).

3 Results

3.1 Cultivation experiment

The concentrations of nitrate and silicate declined rapidly over the course of the experiment (Fig. 1). After eight days, silicate decreased to concentrations below 2 µmol L^{-1} a threshold known to limit diatom dominance in phytoplankton (Egge and Aksnes, 1992), while inorganic nitrogen (nitrate, nitrite, and ammonium) became limiting (<0.5 µmol L^{-1} , POC:PON >8-9 DIN:DIP<16) only in the axenic culture. DIN:DIP ratios far below 16, or DIN concentrations below 2 µmol L^{-1} have been described as indication for DIN limitation (Pedersen and Borum, 1996), as well as POC:PON ratios >9 (Geider and La Roche, 2002). Phosphate was not potentially growth limiting with molar DIN to PO_4 ratios consistently far below 16 (Redfield, 1934) and concentrations around 15 µmol L^{-1}. Typically phosphate concentrations below 0.3 µmol L^{-1} are typically considered limiting (e.g. Haecky and Andersson, 1999). Regeneration of ammonium and phosphate were important by the start of the stationary phase as seen by increasing concentrations of both nutrients and showed higher concentrations in the bacteria enriched experiments compared to the axenic cultures (Fig. 1a,b). Ammonium concentrations were consistently higher, and nitrate was removed more slowly in the presence of bacteria, especially during the exponential phase. DOC values were very high from the start (approx. 2-4 mmol L^{-1}) and remained largely constant throughout the experiment (Table A8).

The diatom *Chaetoceros socialis* grew exponentially in both treatments until day 8 before reaching a stationary phase with declining cell numbers (Fig. 2). The growth rate of the axenic culture (0.36 d^{-1}) was slightly lower than in the treatment with bacteria present (0.42 d^{-1}) during the exponential phase. Algal cellular abundance was higher in the bacteria-enriched cultures. Towards the end of the exponential phase, the diatom started to form noticeable aggregates in cultures with bacteria present,

https://doi.org/10.5194/bg-2020-314
Preprint. Discussion started: 4 September 2020

but only to a limited extend in the axenic cultures. Such aggregate formation with associated EPS production is typical for *C. socialis*. With the onset of the stationary phase in the bacteria-enriched cultures about 30% of the cells formed biofilms on the walls of the cultivation bottles (estimated after sonication treatment). Bacteria (Fig. 2) continued to grow throughout the entire experiment, but growth rates slowed down from 0.9 to 0.6 after day 8. In the axenic cultures, bacterial numbers increased after 8 days, but abundances remained two order of magnitude below the bacteria enriched cultures and effectively axenic over the experimental incubation period. The maximum photosynthetic quantum yield (Fv/Fm) as a proxy of photosynthetic fitness (high QY) increased from approx. 0.62 to 0.67 in the exponential phase and decreased to approx. 0.62 in the bacteria-enriched treatment after 8 days and to approx. 0.58 in the axenic treatments (Table A8).

During algal exponential growth, POC and PON concentrations followed changes in algal abundances increasing four, seven, and 19-fold respectively, within 8 days (Fig. 2a, 3). Interestingly, with the beginning of the stationary phase, POC and PON continued to increase in the bacteria-enriched cultures, while their concentrations stayed constant (POC), or decreased (PON) in axenic cultures. POC and PON concentrations were consistently higher (1.2 times POC, 1.4 times PON) in bacteria-enriched cultures during the exponential phase. gC : gN ratios decreased in both cultures, but increased again after 11 days in the axenic culture. Chlorophyll *a* concentrations also increased exponentially over the first eight days in both treatments, and thereafter decreased within the stationary phase in the axenic cultures. In contrast, cell numbers remained nearly constant in the bacteria-enriched cultures, before declining at the last sampling day.

Overall, both experimental cultures showed similar growth dynamics until day 8, with silicate becoming limiting for both treatments and nitrogen only limiting in axenic cultures. Algal growth with bacteria present was slightly, but consistently higher during this phase. After eight days, algae growth stopped in both treatments, but nitrogen and carbon were continuously assimilated in bacteria-enriched cultures. Axenic cultures started to degrade chlorophyll, while it stayed the same in bacteria-enriched cultures. Algal abundances in the bacteria-enriched treatment at the end of the experiment were ca 30% higher due to biofilm formation, and considerably more carbon (2x total POC, or 10-20% per cell) and nitrogen (3x total PON) per cell had been assimilated, and considerably more chlorophyll (2-3x total chlorophyll) produced at day 16. Cell size differences were not detectable (ca 4µm diameter, Table A8). POC to PON ratios increased after 11 days in axenic cultures to maximum values of 7.2 and 1.3 mmol L^{-1}, respectively, but showed no change in bacteria-enriched cultures. POC to Chl ratios were comparable in both treatments (Fig. 4). Assuming axenic N fixation was mostly based on new production (nitrate as N source), while the algal N fixation in bacterial enriched treatments was based on new and regenerated (ammonium as N source) production, two third of the production was based on regenerated production (f-ratio = 0.31).

3.2 Modelling

A comparison of the traditional G98 model with the extended model allowed to estimate the importance of bacterial DIN regeneration and Si co-limitations for describing the experimental growth dynamics. The extended model led to no improved fit to the axenic experiment ($RMSE_{G98}$ = 3.8 $RMSE_{EX}$ = 3.9, Fig. 6). The real strength of the extended model was in representing

https://doi.org/10.5194/bg-2020-314
Preprint. Discussion started: 4 September 2020


Biogeosciences Discussions

growth dynamics with bacteria present (Fig. 7). Here, the fitted lines mostly overlapped with the range of measured data and the RMSE was reduced by 60% from $RMSE_{G98}$ = 6.4 down to $RMSE_{EX}$ = 2.2.

Both, the G98 and extended model fits of the axenic experiment were equally good for POC and PON with a slightly lower modelled growth rate. However, both models had limitations in modelling chlorophyll production, which was underestimated by about 50% at the onset of the stationary phase (Fig. 4c). The degradation of chlorophyll *a* in the stationary phase was not modelled either (Fig. 4c). The bacteria-enriched experiment was poorly modelled without consideration of silicate limitation or regenerated production specifically towards the end of the exponential phase and during the stationary phase. Maximum POC, PON and Chl values were 2-3 times lower using the G98 model (Fig. B3). In addition, the start of the stationary phase in the bacteria-enriched experiment was estimated 3 days too late via G98, even though modelled DIN was depleted 2 days too soon (Fig. B3). Under axenic conditions, where silicate limitation does not play a major role the G98 model appears sufficient.

The extended model allowed representing detailed dynamics in a bacteria influenced system such as the responses to silicate limitation with a decrease in POC production, continued PON production, and the stagnation of Chl synthesis (Fig. 4). Apart from the lag phase, the mass ratios of C:N and C:Chl were represented accurately (Fig. 4). The model fits without the separate carbon excretion term (x_f) was almost identical to the model with excretion, indicating the importance of the high background dissolved organic matter (DOM) concentrations, rather than excreted DOM for the regenerated ammonium, and the lack of significant aggregation of excreted DOM (identical $RMSE_{Ex}$ of 2.2).

Fine scale DIN dynamics caused by ammonium – nitrate interactions were represented well (Fig. 5a). However, at the onset of the stationary phase, ammonium concentrations of the model were one order of magnitude lower than in the experiment, showing a main weakness of the model (Fig. 5c). The silicate uptake is highly simplified using simple Monod kinetics, with too high modelled values in the stationary phase and a too quick depletion in the start (Fig. 5d). Carbon excretion (x_f) did not have any effect on the model fit to nutrients.

The sensitivity analysis (Fig. B1, Table A1) revealed that the extended model was most sensitive to R^C (max sensitivity >1). R^C is part of the original G98 model, showing that none of the added parameters was more complex than any of the original model parameters. Hence, the added complexity of the extended model does not create a strong new sensitivity. The most sensitive added parameter were the maximum silicate uptake rate (V_{max}) and remineralisation rates (rem, rem_d) with values of the sensitivity analysis reaching ca 0.5, which is comparable to other sensible parameters of the original G98 model (shape factor for photosynthesis (n), I, Θ^N_{max}). The most affected model output by R^C and n was the DIN concentration.

4 Discussion

The experimental incubations represented typical spring bloom dynamics for coastal Arctic systems, including an initial exponential growth phase terminated by N and Si limitation and the potential for an extended growth period via regenerated production. Our model incorporating these results was able to reflect these dynamics by adding NH_4-NO_3-$Si(OH)_4$ co-

https://doi.org/10.5194/bg-2020-314
Preprint. Discussion started: 4 September 2020

limitations and bacterial NH_4 regeneration to the widely used G98 model. In addition, bacteria-algae interactions and DOC and biofilm dynamics were important in the experiment, but those were not crucial for quantitatively modelling algal C:N:Chl quotas.

4.1 Silicon-nitrogen regeneration

Spring phytoplankton dynamics in Arctic and sub-Arctic coastal areas is typically characterised by an initial exponential growth of diatoms, followed by peaks of other taxa (like *Phaeocystis pouchetii*) soon after the onset of silicate limitation (Eilertsen et al. 1989). Thus a shift in species composition for the secondary bloom is linked to silicate limitation prior to final bloom termination caused by inorganic nitrogen limitation. The secondary bloom was extended in time by bacterial regeneration of ammonium, allowing regenerated production to contribute about 69% of the total production (f-ratio=0.31) even during a diatom dominated scenario in our experimental incubation. The presence of bacteria and thus regenerated production allowed algae growth to continue 8 days after silicate became limiting (Figs. 1,2 & 3), nearly doubling the growth period similar to observations in the field (e.g. Legendre and Rassoulzadegan, 1995; Johnson et al., 2007). This extended production shows clearly that bacterial remineralisation is crucial to successfully model spring bloom dynamics, especially near bloom termination. Many biogeochemical models used in the Arctic include remineralisation, but rely on fixed or temperature dependent rates and do not consider them bacteria-dependent (MEDUSA, LANL, NEMURONPZD, see Table 1). While this simplification allows modelling regenerated production, using bacteria-independent remineralisation rates it does have limitations under spring bloom scenarios, where bacteria biomass can vary over orders of magnitudes (e.g. Sturluson et al., 2008) as also seen in our experimental study.

Regenerated production is significant in polar systems and our estimated experimental f-value of 0.31 is slightly below the average for polar systems (Harrison and Cota, 1990, mean f-ratio=0.54). The absence of vertical PON export in our experiment may explain the above average fraction of regenerated production. In the ocean environment, regenerated production is also affected by vertical export (sedimentation) and grazing which are not represented in the experimental incubations. Via sedimentation, a fraction of the bloom either in the form of direct algal sinking of fecal pellets is typically exported to deeper water layers, reducing the potential for N regeneration within the euphotic zone (e.g. Keck and Wassmann, 1996). Larger zooplankton grazing can lead to increased export of PON via fecal pellet aggregation, or diel vertical migration (Banse, 1995). In contrast, bacterial death by microflagellate grazing and viral lysis may supply additional nutrients, or DON available for N regeneration in the euphotic zone (e.g. Goldman and Caron, 1985), which potentially leads to an overestimation of regenerated production. Hence, ecosystem scale models will need to consider these dynamics regarding bacterial abundances, microbial networks and particle export in addition to bacterial remineralization order to model realistic ammonium regeneration in the euphotic zone.

Bacteria-mediated silicate regeneration is absent from the modeling approach, as indicated by the identical silicate concentrations in both treatments (Fig. 1). In the environment silicate dissolution is, in fact, mostly described as an abiotic process with temperature as the main control, and a minor contribution by bacterial remineralisation (Bidle and Azam, 1999).

https://doi.org/10.5194/bg-2020-314
Preprint. Discussion started: 4 September 2020

Our experiment indicates that silicate dissolution for *Chaetoceros socialis* was negligible at cold temperatures and time scale of the incubations and typical for bloom durations and residence times of algae cells in the euphotic zone (Eilertsen et al., 1989, Keck and Wassmann, 1996). We conclude that silicate dissolution in coastal Arctic systems happens most likely in the sediment or deeper water layers and is only supplied via mixing in winter. In Antarctica substantial silicate dissolution has been observed but not in the upper 100m, which has been related to the low temperatures (Nelson and Gordon, 1981) in agreement with our conclusion. Hence, modelling silicate regeneration in the euphotic zone is not necessary in these systems.

4.2 Algal growth response to Si and N limitation

The response of diatoms to Si or N limitation is based on different dynamics and different roles of N and Si in diatom growth. N is needed for proteins and nucleic acids, while Si is only needed for frustule formation, mostly during a specific time in the cell cycle (G2 and M phase, Hildebrand, 2002). Once N is limiting, growth rapidly stops (Geider et al. 1998). In the case of SI limitation, however, growth can continue with a slower rate if N is still available (Werner, 1978). Several studies found a reduced growth rate (Hildebrand, 2002; Gilpin, 2004), but unaffected nitrogen assimilation under silicate limitation (Hildebrand 2002, Claquin et al., 2002) in accordance with our study. Claquin et al. (2002) found variable Si:C and Si:N ratios and highly silicified cells under nitrogen limitation, indicating uncoupled Si and N:C metabolism.

Nitrogen is a crucial element as part of amino acids and nucleic acids, which are necessary for cell activity and growth. If N becomes limiting major cellular processes are affected and growth or chlorophyll synthesis is not possible. Photosynthesis can continue for a while leading to carbon overconsumption (Schartau et al., 2007). A part of the excess carbon can be stored as intracellular reserves, and a part is excreted as DOC, which may aggregate as extracellular polymeric substances (EPS), contributing to the total POC pool. The excess carbon can potentially be toxic for the algae and excretion and extracellular degradation by bacteria may be crucial for algal survival (Christie-Oleza et al., 2017). Quantitatively, N limitation is well modelled by G98 under axenic conditions, if only one nitrogen source plays a role. However, under longer nitrogen starvation times or higher light intensities, alternative models that include carbon excretion and aggregation (Schartau et al., 2007) or intracellular storage in reserve pools (Ross & Geider 2009) might be needed. Our growth experiment shows clearly, that C:N ratios are not fixed and variable quotas are needed. Vichi et al. (2007) estimated that Carbon based models may underestimate net primary production (NPP) by 50%, arguing for the importance of quota based models (Fransner et al., 2018). However, most ecosystem scale models are simplified by using fixed C:N ratios (Table 1).

The type of inorganic nitrogen available also affects nitrogen uptake. Ammonium is typically preferred over nitrate and can inhibit or reduce nitrate uptake over certain concentrations. The dynamics are mostly controlled by intracellular processes, such as glutamate feedbacks on nitrogen assimilation, cost for nitrate conversion to ammonium, or lower half saturation constants of ammonium transporters (Flynn et al., 1997). The most accurate representation of these dynamics are given in the ANIM model by Flynn et al. (1997), but the model is too complex for implementations in larger ecosystem models. The number of parameters is difficult to tune with the typically limited availability of measured data and its complexity makes it also computationally costly to scale the models up. Typically, modelling ammonium-nitrate interactions by different half-

https://doi.org/10.5194/bg-2020-314
Preprint. Discussion started: 4 September 2020

saturation constants and inhibition of nitrate uptake by ammonium appears sufficient (e.g. BFM, LANL, NEMURO, Table 1) and has been adapted in our model.

Silicate limitation affects mainly the cell cycle. Without silicate, diatoms cannot form new frustules needed for forming new cells. Nitrogen assimilation, photosynthesis, and synthesis of proteins and nucleic acids can continue at lower rates (Werner, 1978). Cell size is limited by the frustules, but cells may become more nutritious (higher N:C ratio), or simply excrete more DOM, which may aggregate and contribute to the PON and POC pools. A detailed cell-cycle based model has been suggested by Flynn (2001), but its complexity remains too high for ecosystem scale models. In ecosystem scale models Si limitation is modelled in various simplifications, such thresholds for absence (MEDUSA), and reduced Si dependent production (e.g. BFM, MEDUSA, SINMOD, Table 1), or Si:N ratio scaled production (NEMURO, Table 1). We modelled the response of diatom growth to silicate limitation by reducing photosynthesis by 80% and a stop of chlorophyll synthesis under a certain threshold, based on experimental studies (Werner, 1978) and in accordance to other ecosystem scale approaches. We suggest that this extension is more accurate than the typical threshold based dynamics, with one limiting nutrient controlling the growth equally for POC and chl production (e.g. SINMOD by Wassmann et al., 2006; BFM by Vichi et al., 2007), while still keeping the complexity low.

4.3 Importance of algae-bacteria interactions and DOC excretion

As described above, N or Si limitation can lead to excretion of DON and DOC, which can aggregate as EPS and be available for bacterial regeneration of ammonium. For including EPS dynamics in the model additional data would be needed. However, the importance of EPS formation is clear in the end of the bacteria-enriched experiment. Firstly, a biofilm was clearly visible containing about 30% of the algae cells. Secondly, POC and PON concentrations increased, while cell numbers and sizes stayed constant, showing that the additional POC and PON was most likely part of an extracellular pool. Silicate limitation could be one trigger for enhanced exudation. Interestingly, algae – bacteria interactions can be species specific with specific organic molecules excreted by the algae to attract specific beneficial bacteria (Mühlenbruch et al., 2018). Thereby bacteria are crucial for recycling ammonium, but also to degrade potentially toxic exudates (Christie-Oleza et al., 2017).

In the axenic experiment, Carbon excretion after Carbon overconsumption could be expected after Schartau et al. (2007), but no indications, such as biofilm formation, or increased POC per cell were found. This indicates that carbon overconsumption has been of minor importance likely due to the low light levels. An alternative explanation is that bacteria and potentially chemotaxis are important controls on algal carbon excretion (Mühlenbruch et al., 2018). Overall, DOM excretion and EPS dynamics appear to play a minor role in quantitatively modelling C:N:Chl quotas in our experiment, with identical RMSEs (2.2) for a model run with and without the excretion term x_f. However, in systems with less allochthonous DOM inputs, such as open oceans compared to coastal sites, these dynamics will most likely play a more important role.

https://doi.org/10.5194/bg-2020-314
Preprint. Discussion started: 4 September 2020

4.4 Considerations in a changing climate

Due to a rapid changing climate, especially in Arctic coastal systems, the dynamics addressed in this study will change (Tremblay and Gagnon 2009). With warmer temperatures, heterotrophic activities, and thereby bacterial recycling will increase (Kirchman et al., 2009). Our study showed that regenerated production is crucial for an extended spring bloom. Hence, higher heterotrophic activities may lead to extended blooms (higher f-ratio). At the same time, higher temperatures and increased precipitation will lead to stronger and earlier stratified water columns, which will lead to less nutrients reaching the surface by winter mixing, reducing new production (lower f-ratio)(Tremblay and Gagnon, 2009; Fu et al., 2016). Consequently, the phenology of Arctic coastal primary production in a warmer climate will likely be increasingly driven by bacterial remineralization, showing the necessity to include this process into biogeochemical models. An earlier temperature driven water column stratification will also lead to an earlier bloom however with potentially lower light intensities. In this case, less light is available earlier in the Arctic spring season and carbon overconsumption as described by Schartau et al. (2007) may become less important. An earlier phytoplankton bloom can lead to a mismatch with zooplankton grazers (Durant et al., 2007; Sommer et al., 2007), which could decrease the fecal pellet driven vertical export and thereby increase the residence time of POM in the euphotic zone and the potential for ammonium regeneration, making the incorporation of bacterial recycling into ecosystem models even more imporatant as also evident from our experimental data and model output. In fact, global climate change models agree that vertical carbon export are overall decreasing (Fu et al., 2016). Silicate regeneration is thought to be mostly controlled abiotically by temperature (Bidle and Azam, 1999). Thus, increasing temperature and a stronger stratification will allow recycling of silicate in the euphotic zone before sinking out and thus could cause a shift in the algal succession observed during spring with prolonged contributions of diatoms. Thus, a temperature dependent silica dissolution may need to be included for models in a substantially warmer climate in further model developments. Increased precipitation will also lead to increased runoff and allochthonous DOM inputs, increasing the importance of terrestrial DOM degradation and decreasing the relative importance of algal exudate regeneration (Jansson et al., 2008). The high fraction of regenerated production mostly based on allochtonous DOM degradation, the limited role of excreted DOM degradation, low light levels, and the absence of grazing and export fluxes are simplifications of our study, which are, however, expected to be realistic scenarios under climate change. Hence, we suggest that our experiment and model are well suited as a baseline for predictive ecosystem models investigating the impacts of climate change on coastal Arctic spring blooms. However, climate change may lead to shifts in algae communities with non-silicifying algae dominating over diatoms (e.g. Falkowski and Oliver, 2007), reducing the importance of silicate limitation. Thus, conducting similar experiments and modelling exercises with a wider range of algal taxa and different temperature and nutrient regimes is suggested.

https://doi.org/10.5194/bg-2020-314
Preprint. Discussion started: 4 September 2020

Acknowledgements

The project was supported by ArcticSIZE - A research group on the productive Marginal Ice Zone at UiT (project number 01vm/h15). We want to thank Paul Dubourg and Elzbieta Anna Petelenz-Kurdziel for the help with Nutrient and POC/PON analyses. DOC analyses was supported through a Fulbright Distinguished Scholar Award to HRH.

Authors contributions

TRV designed the experiment with contributions by RG and ML. TRV isolated and identified the cultures. ML performed the experiment with contributions of TRV and UD. RH measured DOC and SK measured the Nutrients. The other parameters where measured by ML and TRV. TRV programmed the model with contributions of CV, ST and DvO. TRV wrote the manuscript with contributions from all co-authors.

Data availability

The experimental data are archived at DataverseNO under the doi number doi.org/10.18710/VA4IU9. The Rscripts for the model are available from the corresponding author upon request.

Competing interests

The authors declare that they have no conflict of interest.

References

Al Khudary, R., Stößer, N. I., Qoura, F., and Antranikian, G.: Pseudoalteromonas arctica sp. nov., an aerobic, psychrotolerant, marine bacterium isolated from Spitzbergen, Int. J. Syst. Evol. Microbiol., 58, 2018-2024, 2008.

Altschul, S. F., Gish, W., Miller, W., Myers, E. W. and Lipman, D. J.: Basic local alignment search tool, J. Mol. Biol., 215, 403-410, 1990.

Amin, S. A., Parker, M. S., and Armbrust, E. V.: Interactions between diatoms and bacteria, Microbiol. Mol. Biol. Rev., 76(3), 667-684, 2012.

Amin, S. A., Hmelo, L. R., Van Tol, H. M., Durham, B. P., Carlson, L. T., Heal, K. R., Morales, R. L., Berthiaume, C. T., Parker, M. S., Djunaedi, B., Ingalls, A. E., Parsek, M. R., Moran, M. A., and Armbrust, E.V.: Interaction and signalling between a cosmopolitan phytoplankton and associated bacteria, Nature, 522, 98-101, 2015.

Andersen, R. A., and Kawachi, M.: Microalgae isolation techniques, in: Algal culturing techniques, edited by: Andersen, R. A., Elsevier, 83, 2005.

https://doi.org/10.5194/bg-2020-314
Preprint. Discussion started: 4 September 2020

Banse, K.: Zooplankton: pivotal role in the control of ocean production: I. Biomass and production, ICES J. Mar. Sci., 52, 265-277, 1995.

Bertani, G.: Lysogeny at mid-twentieth century: P1, P2, and other experimental systems, J. Bacteriol., 186, 595-600, 2004.

Bidle, K. D., and Azam, F.: Accelerated dissolution of diatom silica by marine bacterial assemblages, Nature, 397, 508-512, 1999.

Booth, B. C., Larouche, P., Bélanger, S., Klein, B., Amiel, D., and Mei, Z. P.: Dynamics of Chaetoceros socialis blooms in the North Water, Deep Sea Res. Part II Top. Stud. Oceanogr., 49, 5003-5025, 2002.

Burdige, D.J., and Homstead, J.: Fluxes of dissolved organi carbon from Chesapeake Bay sediments. Geochim. Cosmochim. Acta, 58, 3407-3424, 1994.

Christie-Oleza, J. A., Sousoni, D., Lloyd, M., Armengaud, J., and Scanlan, D. J.: Nutrient recycling facilitates long-term stability of marine microbial phototroph–heterotroph interactions, Nat Microbiol, 2, 17100, 2017.

Claquin, P., Martin-Jézéquel, V., Kromkamp, J. C., Veldhuis, M. J. W., and Kraay, G. W.: Uncoupling of Silicon Compared With Carbon and Nitrogen Metabolisms and the Role of the Cell Cycle in Continuous Cultures of Thalassiosira Pseudonana (Bacillariophyceae) Under Light, Nitrogen, and Phosphorus Control, J. Phycol., 38(5), 922–930, 2002.

Degerlund, M., and Eilertsen, H. C.: Main species characteristics of phytoplankton spring blooms in NE Atlantic and Arctic waters (68–80 N), Estuaries Coast, 33, 242-269, 2010.

Dortch, Q.: The interaction between ammonium and nitrate uptake in phytoplankton. Mar. Ecol. Prog. Ser., Oldendorf, 61, 183-201, 1990.

Durant, J. M., Hjermann, D. Ø., Ottersen, G., and Stenseth, N. C.: Climate and the match or mismatch between predator requirements and resource availability, Climate research, 33, 271-283, 2007.

Egge, J. K., and Aksnes, D.L.: Silicate as regulating nutrient in phytoplankton competition, Mar. Ecol. Prog. ser., 83, 281-289, 1992.

Eilertsen, H. C., and Frantzen, S.: Phytoplankton from two sub-Arctic fjords in northern Norway 2002–2004: I. Seasonal variations in chlorophyll a and bloom dynamics, Mar. Biol. Res., 3, 319-332, 2007.

Eilertsen, H. C., Taasen, J. P., and WesIawski, J. M.: Phytoplankton studies in the fjords of West Spitzbergen: physical environment and production in spring and summer, J. Plankton Res., 11, 1245-1260, 1989.

Falkowski, P. G., and Oliver, M. J.: Mix and match: how climate selects phytoplankton, Nat. Rev. Microbiol., 5, 813-819, 2007.

Field, C. B., Behrenfeld, M. J., Randerson, J. T., and Falkowski, P.: Primary production of the biosphere: integrating terrestrial and oceanic components, Science, 281, 237-240, 1998.

Flynn, K. J.: A mechanistic model for describing dynamic multi-nutrient, light, temperature interactions in phytoplankton, J. Plankton Res., 23, 977-997, 2001.

Flynn, K. J.: Modelling multi-nutrient interactions in phytoplankton; balancing simplicity and realism, Prog. Oceanogr., 56, 249-279, 2003.

https://doi.org/10.5194/bg-2020-314
Preprint. Discussion started: 4 September 2020

Flynn, K. J., and Fasham, M. J.: A short version of the ammonium-nitrate interaction model, J. Plankton Res., 19, 1881-1897, 1997.

Flynn, K. J., Fasham, M. J., and Hipkin, C. R.: Modelling the interactions between ammonium and nitrate uptake in marine phytoplankton. Philosophical Transactions of the Royal Society of London, Series B: Biological Sciences, 352, 1625-1645, 1997.

Flynn, K. J.: Nitrate transport and ammonium-nitrate interactions at high nitrate concentrations and low temperature, Mar. Ecol. Prog. Ser., 187, 283-287, 1999.

Flynn, K. J., Marshall, H., and Geider, R. J.: A comparison of two N-irradiance interaction models of phytoplankton growth, Limnol. Oceanogr., 46, 1794-1802, 2001.

Fransner, F., Gustafsson, E., Tedesco, L., Vichi, M., Hordoir, R., Roquet, F., Spilling, K., Kuznetsov, I., Eilola, K., Mörth, C., Humborg, C., and Nycander, J.; Non-Redfieldian Dynamics Explain Seasonal pCO2 Drawdown in the Gulf of Bothnia, J Geophys Res Oceans, 123, 166-188, 2017.

Fritz, M., Vonk, J. E., and Lantuit, H.: Collapsing arctic coastlines, Nat Clim Chang, 7, 6, 2017.

Fu, W., Randerson, J. T., and Moore, J. K.: Climate change impacts on net primary production (NPP) and export production (EP) regulated by increasing stratification and phytoplankton community structure in the CMIP5 models, Biogeosciences, 13, 5151-5170, 2016.

Geider, R., and La Roche, J.: Redfield revisited: variability of C: N: P in marine microalgae and its biochemical basis, European J. Phycol., 37(1), 1-17, 2002.

Geider, R. J., Maclntyre, H. L., and Kana, T. M.: A dynamic regulatory model of phytoplanktonic acclimation to light, nutrients, and temperature, Limnol. Oceanogr., 43, 679-694, 1998.

Gilpin, L.: The influence of changes in nitrogen: silicon ratios on diatom growth dynamics, J. Sea Res., 51, 21–35, 2004.

Goldman, J. C., and Caron, D. A.: Experimental studies on an omnivorous microflagellate: implications for grazing and nutrient regeneration in the marine microbial food chain, Deep Sea Res A, 32, 899-915, 1985.

Guillard, R.L.L.: Culture of phytoplankton for feeding marine invertebrates, in: Culture of Marine Invertebrates Animals, edited by: Smith, W.L., Chanley, M.H., Plenum Press, New York, 29–60, 1975.

Harrison, W. G., and Cota, G. F.: Primary production in polar waters: relation to nutrient availability, Polar Res, 10, 87-104, 1991

Haecky, P., & Andersson, A.: Primary and bacterial production in sea ice in the northern Baltic Sea, Aquat. Microb. Ecol., 20(2), 107-118, 1999.

Hauck, J., Völker, C., Wang, T., Hoppema, M., Losch, M., & Wolf-Gladrow, D. A.: Seasonally different carbon flux changes in the Southern Ocean in response to the southern annular mode, Global Biogeochem Cycles, 27, 1–10, 2013.

Hildebrand, M.: Lack of coupling between silicon and other elemental metabolisms in diatoms, J. Phycol., 38, 841–843, 2002.

Hohn, S.: A model of the carbon:nitrogen:silicon stoichiometry of diatoms based on metabolic processes, PhD thesis, Universit¨at Bremen, Bremen, 43-57, 2009.

https://doi.org/10.5194/bg-2020-314
Preprint. Discussion started: 4 September 2020

Hünken, M., Harder, J., and Kirst, G. O.: Epiphytic bacteria on the Antarctic ice diatom Amphiprora kufferathii Manguin cleave hydrogen peroxide produced during algal photosynthesis, Plant Biology, 10, 519-526, 2008.

Iversen, K. R., and Seuthe, L.: Seasonal microbial processes in a high-latitude fjord (Kongsfjorden, Svalbard): I. Heterotrophic bacteria, picoplankton and nanoflagellates, Polar Biol., 34, 731-749, 2011.

Jacobsen, T. R., and Rai, H.: Comparison of spectrophotometric, fluorometric and high performance liquid chromatography methods for determination of chlorophyll a in aquatic samples: effects of solvent and extraction procedures, Internationale Revue der gesamten Hydrobiologie und Hydrographie, 75, 207-217, 1990.

Jansson, M., Hickler, T., Jonsson, A. and Karlsson, J.: Links between terrestrial primary production and bacterial production and respiration in lakes in a climate gradient in subarctic Sweden, Ecosystems, 11, 367–376, 2008.

Johnson, M., Sanders, R., Avgoustidi, V., Lucas, M., Brown, L., Hansell, D., Moore, M., Gibb, S., Liss, P., and Jickells, T.: Ammonium accumulation during a silicate-limited diatom bloom indicates the potential for ammonia emission events, Mar Chem, 106, 63-75, 2007.

Keck, A., and Wassmann, P.: Temporal and spatial patterns of sedimentation in the subarctic fjord Malangen, northern Norway, Sarsia, 80, 259-276, 1996.

Kim, S. J., Kim, B. G., Park, H. J., and Yim, J. H.: Cryoprotective properties and preliminary characterization of exopolysaccharide (P-Arcpo 15) produced by the Arctic bacterium Pseudoalteromonas elyakovii Arcpo 15, Prep. Biochem. Biotechnol., 46, 261-266, 2016.

Kirchman, D. L.: Uptake and regeneration of inorganic nutrients by marine heterotrophic bacteria, Microbial ecology of the oceans, 2000.

Kirchman, D. L., Morán, X. A. G., and Ducklow, H.: Microbial growth in the polar oceans—role of temperature and potential impact of climate change, Nat. Rev. Microbiol., 7, 451-459, 2009.

Kishi, M. J., Kashiwai, M., Ware, D. M., Megrey, B. A., Eslinger, D. L., Werner, F. E., Noguchi-Aita, M., Azumaya, T., Fujii, M., Hashimoto, S., Huang, D., Iizumi, H., Ishida, Y., Kang, S., Kantakov, G. A., Kim, H., Komatsu, K., Navrotsky, V. V., Smith, S. L., Tadokoro, K., Tsuda, A., Yamamura, O., Yamanaka, Y., Yokouchi, K., Yoshie, N., Zhang, J., Zuenko, Y. I., and Zvalinsky, V. I.: NEMURO – a lower trophic level model for the North Pacific marine ecosystem, Ecol. Model., 202, 12–25, 2007.

Le Quéré, C., Andrew, R. M., Canadell, J. G., Sitch, S., Korsbakken, J. I., Peters, G. P., Manning, A. C., Boden, T. A., Tans, P. P., Houghton, R. A., Keeling, R. F., Alin, S., Andrews, O. D., Anthoni, P., Barbero, L., Bopp, L., Chevallier, F., Chini, L. P., Ciais, P., Currie, K., Delire, C., Doney, S. C., Friedlingstein, P., Gkritzalis, T., Harris, I., Hauck, J., Haverd, V., Hoppema, M., Klein Goldewijk, K., Jain, A. K., Kato, E., Körtzinger, A., Landschützer, P., Lefèvre, N., Lenton, A., Lienert, S., Lombardozzi, D., Melton, J. R., Metzl, N., Millero, F., Monteiro, P. M. S., Munro, D. R., Nabel, J. E. M. S., Nakaoka, S.-I., O'Brien, K., Olsen, A., Omar, A. M., Ono, T., Pierrot, D., Poulter, B., Rödenbeck, C., Salisbury, J., Schuster, U., Schwinger, J., Séférian, R., Skjelvan, I., Stocker, B. D., Sutton, A. J., Takahashi, T., Tian, H., Tilbrook, B., van der Laan-Luijkx, I. T., van

https://doi.org/10.5194/bg-2020-314
Preprint. Discussion started: 4 September 2020

der Werf, G. R., Viovy, N., Walker, A. P., Wiltshire, A. J., and Zaehle, S.: Global carbon budget 2016, Earth Syst Sci Data, 8(2), 605-649, 2016.

Legendre, L., and Rassoulzadegan, F.: Plankton and nutrient dynamics in marine waters, Ophelia, 41, 153-172, 1995

Lima, I. D., Olson, D. B., and Doney, S. C.: Intrinsic dynamics and stability properties of size-structured pelagic ecosystem models, J. Plankton Res., 24, 533-556, 2002.

Loebl, M., Colijn, F., van Beusekom, J. E., Baretta-Bekker, J. G., Lancelot, C., Philippart, C. J., Rousseau, V., and Wiltshire, K. H.: Recent patterns in potential phytoplankton limitation along the Northwest European continental coast, J. Sea Res., 61, 34-43, 2009.

Ma, L. Y., Chi, Z. M., Li, J., and Wu, L. F.: Overexpression of alginate lyase of Pseudoalteromonas elyakovii in Escherichia coli, purification, and characterization of the recombinant alginate lyase, World J. Microbiol. Biotechnol., 24, 89-96, 2008.

Martin-Jézéquel, V., Hildebrand, M., and Brzezinski, M. A.: Silicon Metabolism in Diatoms : Implications for Growth, J. Phycol., 36, 821–840, 2000.

Moore, J. K., Doney, S. C., and Lindsay, K.: Upper ocean ecosystem dynamics and iron cycling in a global three-dimensional model, Global Biogeochem Cycles, 18, 2004.

Moore, C. M., Mills, M. M., Arrigo, K. R., Berman-Frank, I., Bopp,L., Boyd, P. W., Galbraith, E. D., Geider, R. J., Guieu, C., Jac-card, S. L., Jickells, T. D., La Roche, J., Lenton, T. M., Ma-howald, N. M., Maranon, E., Marinov, I., Moore, J. K., Nakat-suka, T., Oschlies, A., Saito, M. A., Thingstad, T. F., Tsuda, A.,and Ulloa, O.: Processes and patterns of oceanic nutrient limitation, Nat Geosci, 6, 701-710, 2013.

Mühlenbruch, M., Grossart, H. P., Eigemann, F., and Voss, M.: Mini-review: Phytoplankton-derived polysaccharides in the marine environment and their interactions with heterotrophic bacteria, Environ. Microbiol., 20, 2671-2685, 2018.

Nelson, D. M., & Gordon, L. I.: Production and pelagic dissolution of biogenic silica in the Southern Ocean, Geochim. Cosmochim. Acta, 46(4), 491-501, 1982.

Nelson, D. M., Treguer, P., Brzezinski, M. A., Leynaert, A., and Queguiner, B.: Production and dissolution of biogenic silica in the ocean: revised global estimates, comparison with regional data and relationship to biogenic sedimentation, Glob. Biogeochem. Cycles, 9, 359–372, 1995.

Pedersen, M. F., and Borum, J.: Nutrient control of algal growth in estuarine waters. Nutrient limitation and the importance of nitrogen requirements and nitrogen storage among phytoplankton and species of macroalgae, Mar. Ecol. Prog. Ser., 142, 261-272, 1996

Pella E, Colombo B. Study of carbon, hydrogen and nitrogen determination by combustion-gas chromatography, Microchim Acta. 61, 697–719, 1973.

Redfield, A. C.: On the proportions of organic derivatives in sea water and their relation to the composition of plankton, James Johnstone memorial volume, 176-192, 1934.

Ross, O. N., and Geider, R. J.: New cell-based model of photosynthesis and photo-acclimation: accumulation and mobilisation of energy reserves in phytoplankton, Mar. Ecol. Prog. Ser., 383, 53-71, 2009.

https://doi.org/10.5194/bg-2020-314
Preprint. Discussion started: 4 September 2020

Schartau, M., Engel, A., Schröter, J., Thoms, S., Völker, C., and Wolf-Gladrow, D.: Modelling carbon overconsumption and the formation of extracellular particulate organic carbon, Biogeosciences, 4, 13-67, 2007.

Slagstad, D., Wassmann, P. F., and Ellingsen, I.: Physical constrains and productivity in the future Arctic Ocean, Front Mar Sci, 2, 85, 2015.

Soetaert, K., Petzoldt, T.: Inverse Modelling, Sensitivity and Monte Carlo Analysis in R Using Package FME, J Stat Softw, 33, 1–28, doi: 10.18637/jss.v033.i03, 2010.

Soetaert, K., Petzoldt, T., and Setzer, R. W.: Solving Differential Equations in R: Package deSolve, J Stat Softw, 33, 1548-7660, doi: 10.18637/jss.v033.i09, 2010.

Sommer, U., Aberle, N., Engel, A., Hansen, T., Lengfellner, K., Sandow, M., Wohlers, J., Zollner, E., and Riebesell, U.: An indoor mesocosm system to study the effect of climate change on the late winter and spring succession of Baltic Sea phyto- and zooplankton, Oecologia, 150, 655-667, 2007.

Spilling, K., Tamminen, T., Andersen, T., and Kremp, A.: Nutrient kinetics modeled from time series of substrate depletion and growth: dissolved silicate uptake of Baltic Sea spring diatoms, Marine biology, 157, 427-436, 2010

Stow, C. A., Jolliff, J., McGillicuddy Jr, D. J., Doney, S. C., Allen, J. I., Friedrichs, M. A., Kenneth, A. R., and Wallhead, P.: Skill assessment for coupled biological/physical models of marine systems, J Mar Syst, 76, 4-15, 2009.

Sturluson, M., Nielsen, T. G., and Wassmann, P.: Bacterial abundance, biomass and production during spring blooms in the northern Barents Sea, Deep Sea Res. Part II Top. Stud. Oceanogr., 55, 2186-2198, 2008.

Sverdrup.H.U.: On conditions for the vernal blooming of phytoplankton, Cons. Perm. Int. Expl. Mer, 18, 287-295, 1953.

Teeling, H., Fuchs, B. M., Becher, D., Klockow, C., Gardebrecht, A., Bennke, C. M., Kassabgy, M., Huang, S., Mann, A. J., Waldmann, J., Weber, M., Klindworth, A., Otto, A., Lange,J., Bernhardt, J., Reinsch, C., Hecker, M., Peplies, J., Bockel-mann, F. D., Callies, U., Gerdts, G., Wichels, A., Wiltshire, K.H., Glöckner, F. O., Schweder, T., and Amann, R.: Substrate-controlled succession of marine bacterioplankton populations induced by a phytoplankton bloom, Science, 336, 608-611, 2012.

Teeling, H., Fuchs, B. M., Bennke, C. M., Krueger, K., Chafee, M., Kappelmann, L., Reintjes, G., Waldmann, J., Quast, C., Glöckner, F. O., Lucas, J., Wichels, A., Gerdts, G., Wiltshire, K. H., Amann, R.: Recurring patterns in bacterioplankton dynamics during coastal spring algae blooms, Elife, 5, 2016.

Tezuka, Y.: The C: N: P ratio of phytoplankton determines the relative amounts of dissolved inorganic nitrogen and phosphorus released during aerobic decomposition, Hydrobiologia, 173, 55-62, 1989.

Tremblay, J. É., and Gagnon, J.: The effects of irradiance and nutrient supply on the productivity of Arctic waters: a perspective on climate change, in: Influence of climate change on the changing arctic and sub-arctic conditions, edited by: Nihoul, J. C., J., Kostianoy, A. G., Springer, Dordrecht, 73-93, 2009.

Uitz, J., Claustre, H., Gentili, B., and Stramski, D.: Phytoplankton class-specific primary production in the world's oceans: Seasonal and interannual variability from satellite observations, Global Biogeochem Cycles, 24, 2010.

https://doi.org/10.5194/bg-2020-314
Preprint. Discussion started: 4 September 2020

Van den Meersche, K., Middelburg, J. J., Soetaert, K., Van Rijswijk, P., Boschker, H. T., and Heip, C. H.: Carbon-nitrogen coupling and algal-bacterial interactions during an experimental bloom: Modeling a 13C tracer experiment, Limnol. Oceanogr., 49, 862-878, 2004.

Vichi, M., Pinardi, N., and Masina, S.: A generalized model of pelagic biogeochemistry for the global ocean ecosystem. Part I: Theory, J Mar Syst, 64, 89-109, 2007.

Wassmann, P., Slagstad, D., Riser, C. W., and Reigstad, M.: Modelling the ecosystem dynamics of the Barents Sea including the marginal ice zone: II. Carbon flux and interannual variability, J Mar Syst, 59, 1-24, 2006.

Weitz, J. S., Stock, C. A., Wilhelm, S. W., Bourouiba, L., Coleman, M. L., Buchan, A., Follows, M.J., Fuhrman, J. A., Jover, L., Lennon, J. T., Middelboe, M., Sonderegger, D. L., Suttle, C. A., Taylor, B. P.,Thingstad, T. F., Wilson, W., and Wommack, K. E.: A multitrophic model to quantify the effects of marine viruses on microbial food webs and ecosystem processes, ISME J, 9, 1352-1364, 2015.

Werner, D.: Silicate metabolism, in: The biology of diatoms, edited by: Werner, D., Blackwell Scientific Publications, California, 13, 111-149, 1977.

Werner, D.: Regulation of metabolism by silicate in diatoms, in: Biochemistry of silicon and related problems, edited by: Bendz, G., and Lindqvist, I., Springer, Boston, MA, 149-176, 1978.

Westberry, T. K., Behrenfeld, M. J., Siegel, D. A., Boss, E.: Carbon-based primary productivity modeling with vertically resolved photoacclimation, Global Biogeochem Cycles, 22,1–18, 2008.

Yool, A., and Popova, E. E.: Medusa-1.0: a new intermediate complexity plankton ecosystem model for the global domain, Geosci Model Dev, 4, 381, 2011.

Zambrano, J., Krustok, I., Nehrenheim, E., and Carlsson, B.: A simple model for algae-bacteria interaction in photo-bioreactors, Algal Res, 19, 155-161, 2016.

https://doi.org/10.5194/bg-2020-314
Preprint. Discussion started: 4 September 2020

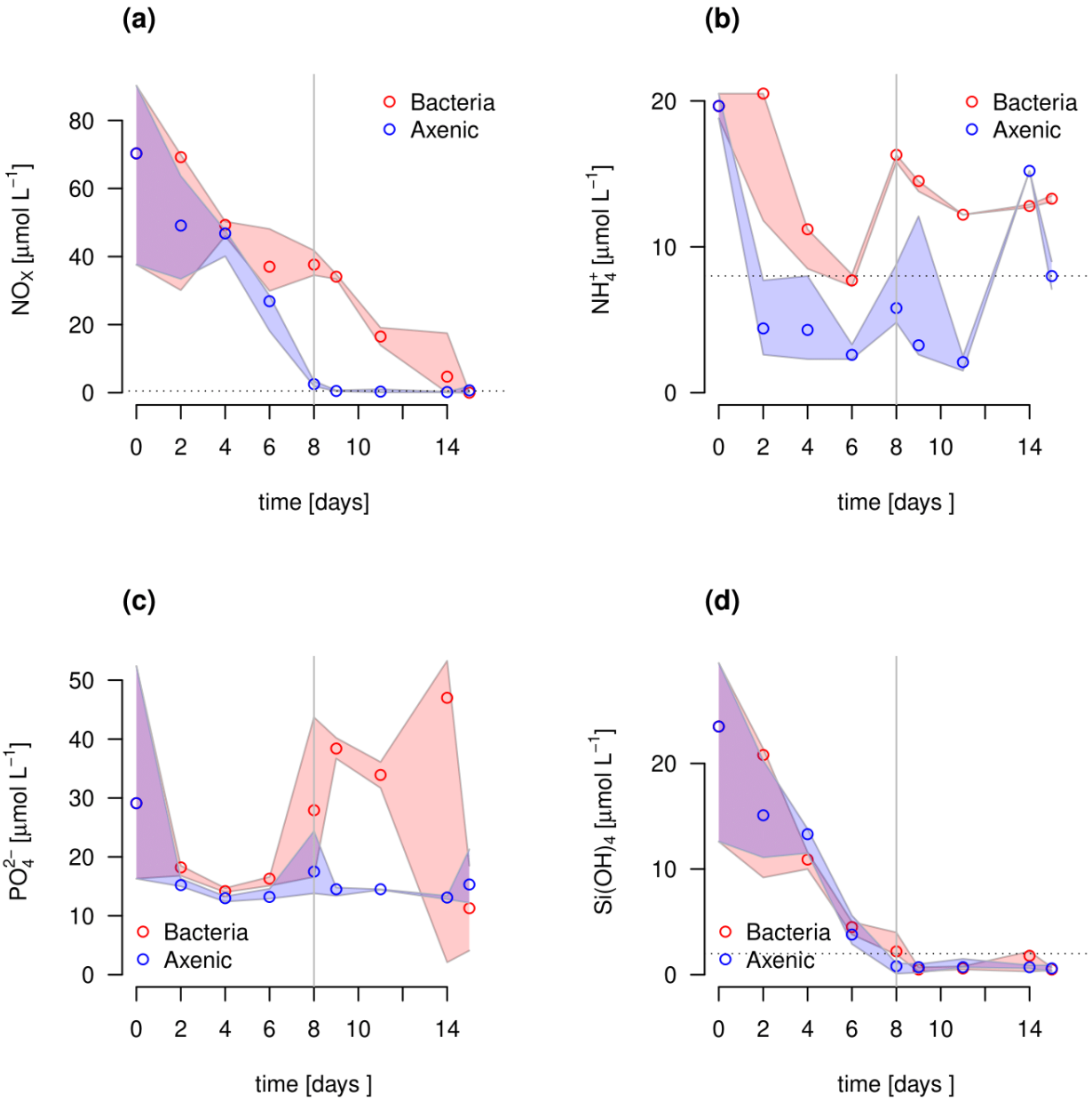

Figure 1. Nutrient measurements over the experimental incubations of a) NO_x, (NO_3^- + NO_2^-) b) NH_4^+, c) PO_4^{2-}, d) Silicate, red circles are axenic cultures and green symbols are bacteria-enriched cultures. Circles show median values (blue = axenic, red = bacteria) and the coloured polygons show the total range of measured data. The grey line shows the beginning of the stationary growth phase of *Chaetoceros socialis* and the dotted horizontal line the threshold under which NO_X or silicate are limiting, or the threshold of NH_4^+ under which nitrate uptake is not inhibited.

https://doi.org/10.5194/bg-2020-314
Preprint. Discussion started: 4 September 2020

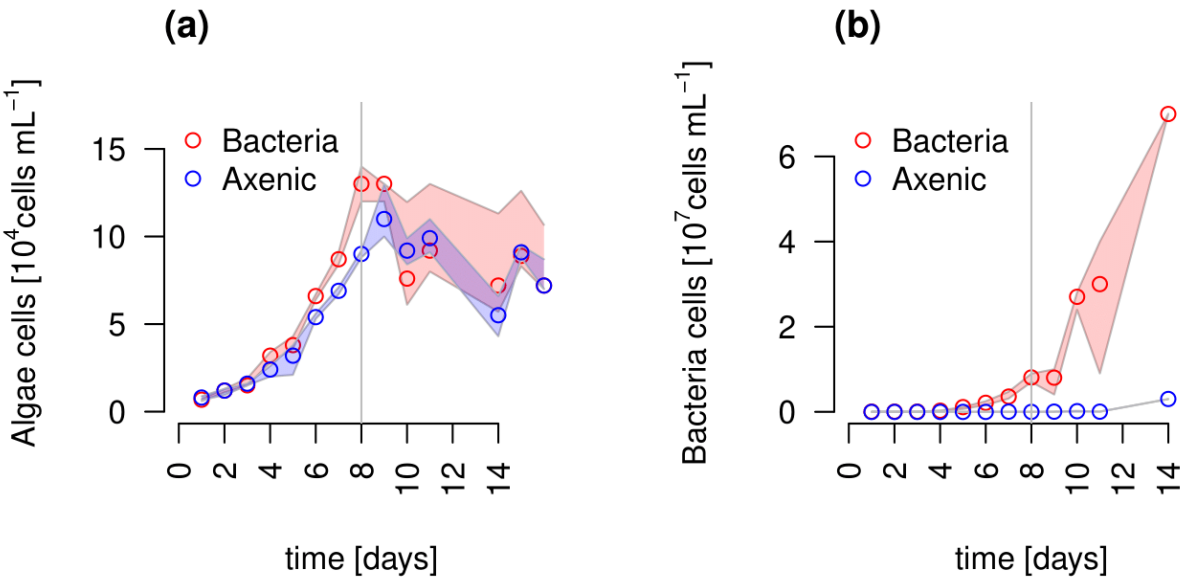

640 Figure 2. Abundances of a) *Chaetoceros socialis* and b) bacteria over the 14 day experimental period. Blue data are from axenic cultures and red from bacteria-enriched cultures. Circles represent median values (blue= axenic, red = bacteria enriched) and the coloured polygons show the total range of measured data (Not visible for bacteria counts in axenic cultures due to very small range). The maximum values of the bacteria enriched experiment includes algae cells in the biofilm (after day 9). The grey line indicates the start of the stationary growth phase of *C. socialis*.

https://doi.org/10.5194/bg-2020-314
Preprint. Discussion started: 4 September 2020

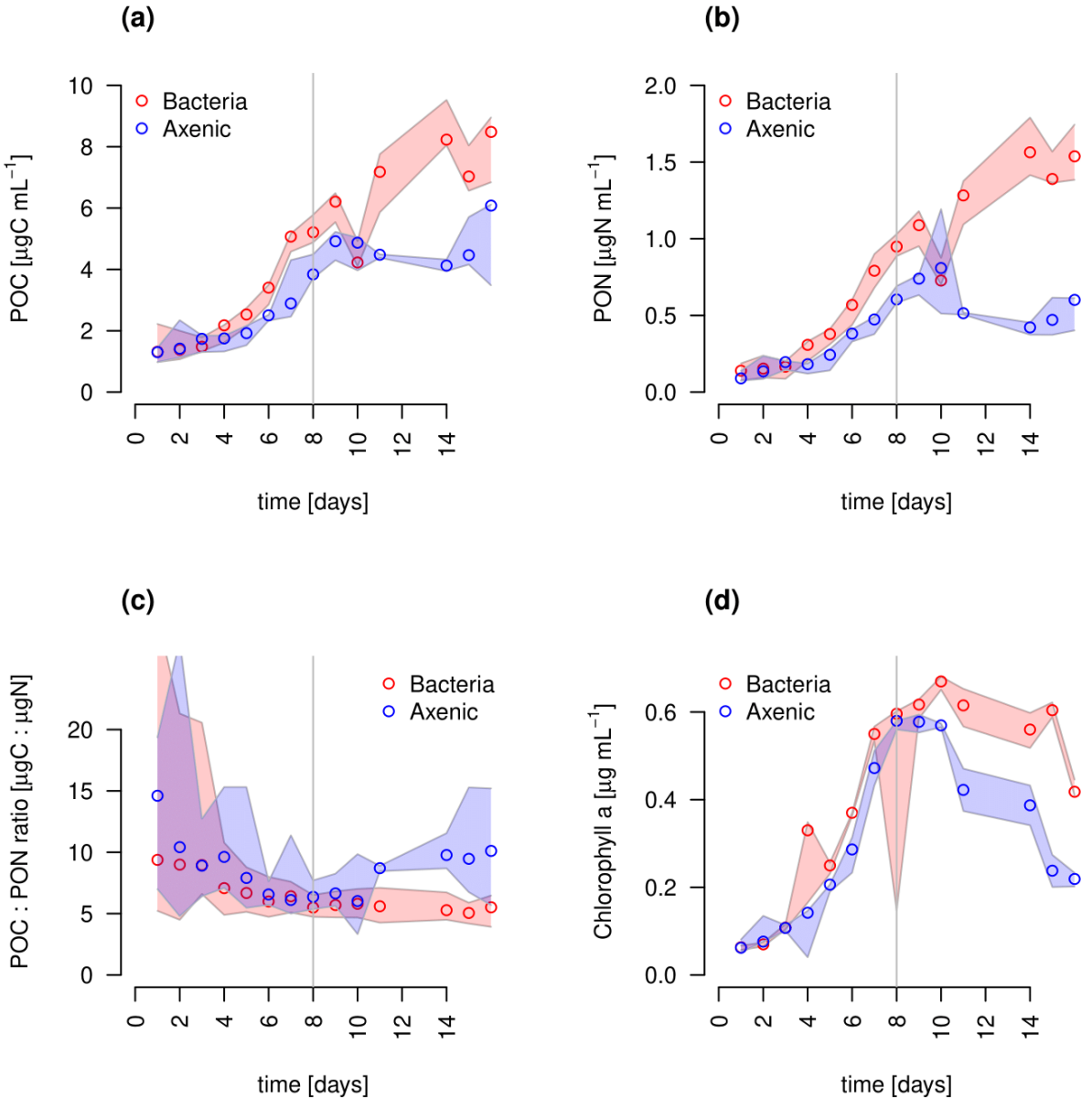

Figure 3. Total particulate organic a) Carbon (POC) b) Nitrogen (PON), c) C : N ratios, and d) Chlorophyll a concentration in experimental cultures. Blue symbols are axenic cultures and red show bacteria-enriched cultures. Circles show median values (blue = axenic, red = bacteria enriched) and the coloured polygons show the total range of measured data. The grey line indicates the start of the stationary phase.

https://doi.org/10.5194/bg-2020-314
Preprint. Discussion started: 4 September 2020

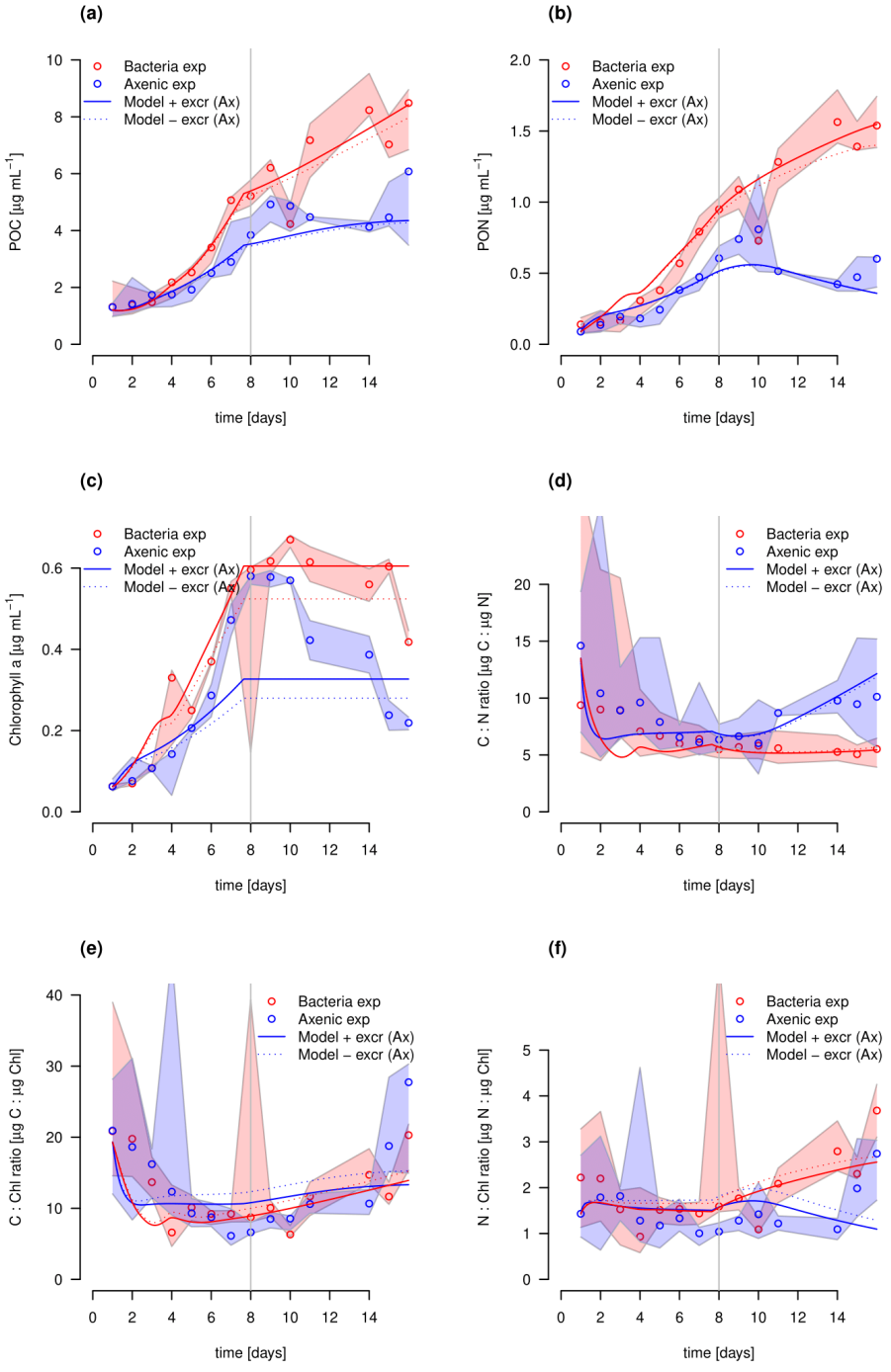

Figure 4: Model fit of the extended model to the axenic (blue) and bacteria enriched (red) experiment. Circles show median values and the coloured polygons show the total range of measured data. Solid lines show the model outputs of a) POC, b) PON, c) Chl, d) C:N, e) C:Chl, and f) N:Chl. Dotted lines show the model fit without the additional Carbon excretion term x_f.

https://doi.org/10.5194/bg-2020-314
Preprint. Discussion started: 4 September 2020

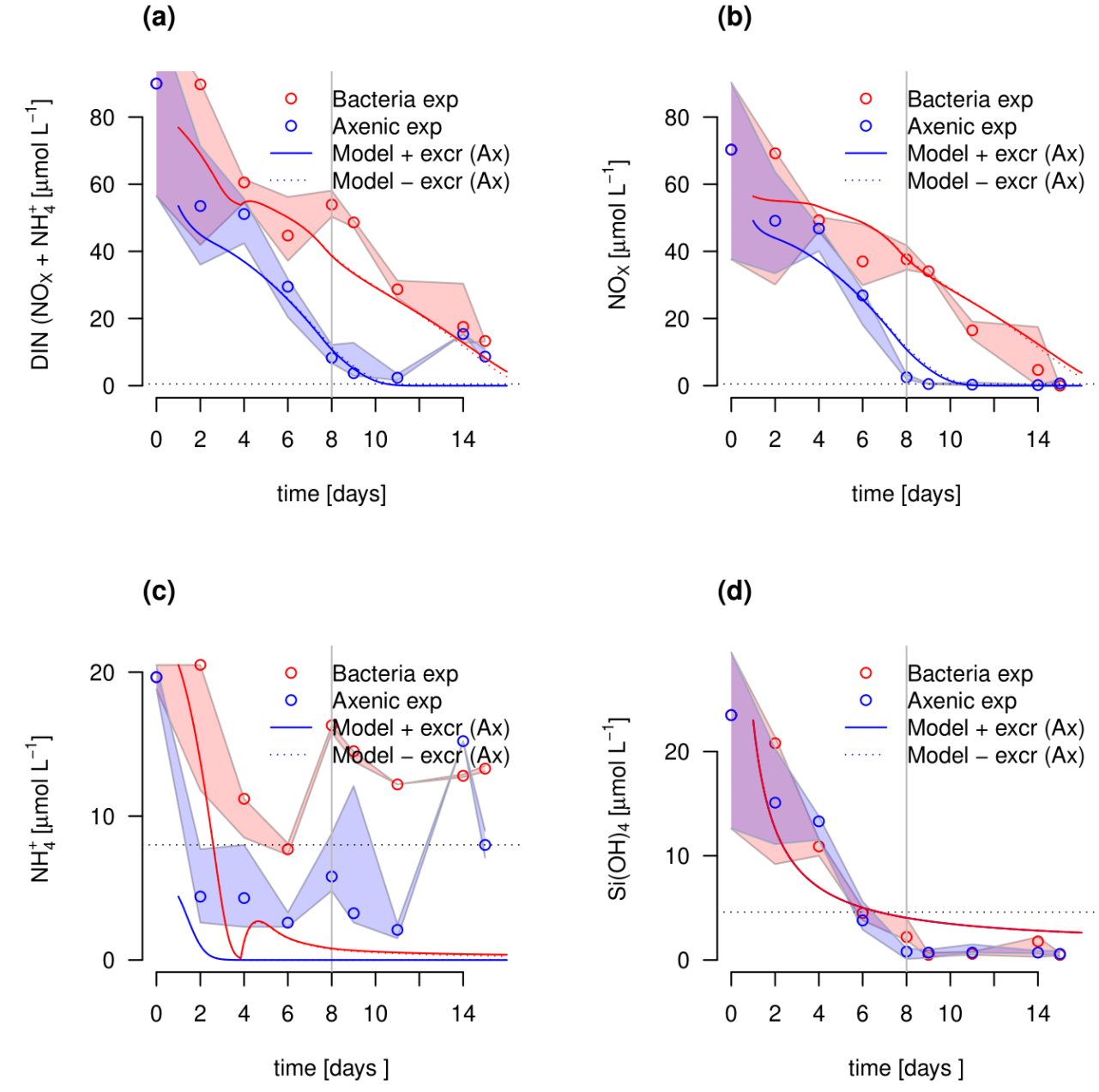

Figure 5: Model fit of the extended model to the axenic (blue) and bacteria enriched (red) experiment. Circles show median values and the coloured polygons show the total range of measured data. Solid lines show the model outputs of a) DIN (NOX and NH4), b) NO_X, c) NH_4, and d) $Si(OH)_4$

https://doi.org/10.5194/bg-2020-314
Preprint. Discussion started: 4 September 2020

Table 1: A comparison of major components contributing to the complexity of different models discussed. #param is the number of parameters. In case of ecosystem models (SINMOD, BFM, MEDUSA, LANL, NEMURO, NPZD only the components representing the components of the current model are considered. REM designates those models that include Remineralisation (Rem), or allow variable ratios of intracellular elements (C:N:Si:P:Fe). The Nutrients considered are given under Nutrients. If DIN is considered as both NH_4 and NO_3, N is shown as N^2. MEDUSA has Fe dependent Si:N ratios, which makes them fixed in the Arctic (fixed*).

Model	Reference	#param	Rem	ratios	Nutrients
		Culture scale			
This model		20[*1]	X	variable	N^2, Si
G98	Geider et al., 1998	10[*2]		variable	N
ANIM	Flynn, 1997	30		variable	N^2
SHANIM	Flynn and Fasham, 1997	23		variable	N^2
Flynn01	Flynn, 2001	54		variable	N^2, Si, P, Fe
		Ecosystem scale			
BFM	Vichi et al., 2007	54	X	variable	N^2, Si, P, Fe
REcoM-2	Hauck et al., 2013	28		variable	N, Si, Fe
MEDUSA	Yool and Popova, 2011	21	X	fixed*	N, Si, Fe
LANL	Moore et al., 2004	15	X	fixed	N^2, Si, P, Fe
NEMURO	Kishi et al., 2007	21	X	fixed	N^2, Si
NPZD	Lima et al., 2002	9	X	fixed	N
SINMOD	Wassmann et al., 2006	12		fixed	N^2, Si

Degrees of freedom after constraints by the measured data are [*1]14 and [*2]6

https://doi.org/10.5194/bg-2020-314
Preprint. Discussion started: 4 September 2020


Biogeosciences Discussions Open Access EGU

Appendix

Tables

Table A1. State variables of the G98 model and the extended model (marked with X) with units and designation if these state variables had been measured in the experiment.

variable	Description	G98	Measured	Unit
DIN	Dissolved inorganic nitrogen	X	X	mgN m^{-3}
pC	Particulate organic carbon	X	X	mgC m^{-3}
pN	Particulate Nitrogen	X	X	mgN m^{-3}
Chl	Chlorophyll a	X	X	mgChl m^{-3}
dSi	Dissolved Silicate			µmol L^{-1}
pSi	Particulate Silicon		X	mgSi m^{-3}
Bact	Bacteria cells		X	10^{r}. cells mL^{-1}
DONr	refractory dissolved organic nitrogen		X	mgN m^{-3}
DONl	labile dissolved organic nitrogen			mgN m^{-3}
NH4	Ammonium		X	µmol L^{-1}
NO3	Nitrate		X	µmol L^{-1}
Q	Particulate N : C ratio			gN gC^{-1}
θ^{C}	Chl to POC ratio			gChl gC^{-1}
θ^{N}	Chl : phytoplankton nitrogen ratio			gChl gN^{-1}

https://doi.org/10.5194/bg-2020-314
Preprint. Discussion started: 4 September 2020

Table A2. parameters of the original G98 model and the model extension with associated units.

parameter		Unit
	G98	
ζ	cost of biosynthesis	gC gN^{-1}
R^C	The carbon-based maintenance metabolic rate	d^{-1}
θ^N_{max}	Maximum value of Chl:N ratio	gChl gN^{-1}
Q_{min}	Min. N:C ratio	gN gC^{-1}
Q_{max}	Max. N:C ratio	gN gC^{-1}
α^{Chl}	Chl-specific initial C assimilation rate	gC m^2 (gChl µmol photons)$^{-1}$
I	Incident scalar irradiance	µmol photons s^{-1} m^{-2}
n	Shape factor for V^N_{max} max photosynthesis	-
K_{no3}	Half saturation constant for nitrate uptake	µmol L^{-1}
P^C_{ref}	Value of max C specific rate of photosynthesis'	d^{-1}
	Extension	
x_f	Carbon excretion fraction	-
K_{si}	Half saturation constant for Si uptake	µmol L^{-1}
V_{max}	maximum Si uptake rate	d^{-1}
s_{min}	minimum Si required for uptake	µmol L^{-1}
rem	remineralisation rate of excreted don	$bact^{-1}$ d^{-1}
rem_d	remineralisation rate of refractory don	$bact^{-1}$ d^{-1}
μ_{bact}	bacteria growth rate	mio. cells mL^{-1} d^{-1}
$bact_{max}$	Carrying capacity for bacteria	mio. cells mL^{-1}
K_{nh4}	Half saturation constant for ammonium uptake	µmol L^{-1}
$nh4_{thres}$	threshold concentration for ammonium uptake	µmol L^{-1}

https://doi.org/10.5194/bg-2020-314
Preprint. Discussion started: 4 September 2020

Table A3. Parameters of the original G98 model and the extended model with initial values used in the model and the lower and upper value constraints used for model fitting, unless the parameter was already defined by the data (measured). The constraints are either based on G98 fits to other diatom species, to present experimental data, or to typical values found in the literature.

parameter	value	lower	upper	constrained by
G98				
ζ	1	1	2	G98
R^C	0.02	0.01	0.05	G98
θ^N_{max}	1.7	measured		Data
Q_{min}	0.05	measured		Data
Q_{max}	0.3	measured		Data
α^{Chl}	0.1	0.075	1	G98
I	100	measured		Data
n	3.7	1	4	G98
K_{no3}	5	2	10	G98
P^C_{ref}	0.8	0.5	3.5	G98
Extension				
x_f	0.06	0.01	0.3	Schartau et al., 2017
K_{si}	10	0.5	10	Werner 1978
V_{max}	0.33	0.32	0.9	Werner 1978
s_{min}	1.82	1.5	6	Werner 1978
rem	5.6	0.1	10	open
rem_d	4.9	0.1	10	open
μ_{bact}	0.04	0.01	0.79	Data
$bact_{max}$	0.015	0.005	0.1	Data
K_{nh4}	4	2	10	open
$nh4_{thres}$	8	0.1	10	open

https://doi.org/10.5194/bg-2020-314
Preprint. Discussion started: 4 September 2020

Table A4. Output of the sensitivity analysis (senFun of the FME package in R).

par	value	scale	L1	L2	Mean	Min	Max	N
				G98				
ζ	1	1	0.20	0.46	0.02	-0.20	2.52	50
R^C	0.02	0.02	0.09	0.13	-0.04	-0.14	0.55	50
θ^N_{max}	1.7	1.7	0.26	0.42	0.11	-1.70	0.59	50
Q_{min}	0.05	0.05	0.06	0.08	-0.04	-0.12	0.22	50
Q_{max}	0.3	0.3	0.41	0.68	-0.31	-3.40	0.26	50
α^{Chl}	0.1	0.1	0.23	0.39	-0.13	-1.90	0.18	50
I	100	100	0.23	0.39	-0.13	-1.90	0.18	50
n	3.7	3.7	0.67	1.71	0.18	-0.53	9.71	50
K_{no3}	5	5	0.03	0.09	0.01	-0.03	0.56	50
P^C_{ref}	0.8	0.8	1.49	3.33	-0.12	-19.00	1.40	50
				Extension				
x_f	0.06	0.06	0.24	0.38	-0.07	-0.37	1.84	50
K_{si}	10	10	0.00	0.00	0.00	0.00	0.00	50
V_{max}	0.33	0.33	0.00	0.00	0.00	0.00	0.00	50
s_{min}	1.82	1.82	0.00	0.00	0.00	0.00	0.00	50
rem	5.6	5.6	0.00	0.00	0.00	0.00	0.00	50
rem_d	4.9	4.9	0.26	0.41	0.26	0.00	1.89	50
μ_{bact}	0.04	0.04	0.00	0.00	0.00	0.00	0.01	50
$bact_{max}$	0.015	0.015	0.00	0.00	0.00	0.00	0.01	50
K_{nh4}	4	4	0.06	0.10	-0.01	-0.18	0.51	50
$nh4_{thres}$	8	8	0.00	0.00	0.00	0.00	0.00	50

https://doi.org/10.5194/bg-2020-314
Preprint. Discussion started: 4 September 2020

Biogeosciences Discussions Open Access EGU

Table A5. Other parameters calculated and used in the model equations

parameter	Description	Unit
P^{C}_{phot}	C-specific rate of photosynthesis	d^{-1}
P^{C}_{max}	Maximum value of P^{C}_{phot} at temperature T	d^{-1}
R^{Chl}	Chl degradation rate constant	d^{-1}
R^{N}	R remineralization rate constant	d^{-1}
V^{C}_{nit}	Phytoplankton carbon specific nitrate uptake rate	gN (gC d)$^{-1}$
V^{C}_{ref}	Value of V^{C}_{max} at temperature T	gN (gC d)$^{-1}$
p_{Chl}	Chl synthesis regulation term	-
μ	specific growth rate of algae	cells d^{-1}

https://doi.org/10.5194/bg-2020-314
Preprint. Discussion started: 4 September 2020


Biogeosciences Discussions Open Access EGU

750 Table A6. Model equations from G98 (Geider et al., 1998) corrected for typographical errors by Ross and Geider (2009) with extensions.

1)	Carbon synthesis	$\frac{dC}{dt} = \left(P^C - \zeta V_N^C - R^C\right)C = \mu C$
2)	Chl synthesis	$\frac{dChl}{dt} = \left(\frac{\rho_{Chl} V_N^C}{\Theta^C} - R_{Chl}\right) Chl$
3)	with	$\rho^{Chl} = \Theta_{max}^N \left[1 - exp\left(-\frac{I}{I_K}\right)\right]$
4)	Nitrogen uptake	$\frac{dN}{dt} = \left(\frac{V_N^C}{Q} - R^N\right) N$
5)	Photosynthesis	$P^C = P_{max}^C \left[1 - exp\left(-\frac{I}{I_K}\right)\right]$
6)	Max. N uptake	$V_N^C = V_{ref}^C \left[\frac{Q_{max} - Q}{Q_{max} - Q_{min}}\right] \frac{DIN}{DIN + K_{no3}}$
7)	with	$V_{ref}^C = P_{ref}^C Q_{max}$
8)		$P_{max}^C = P_{ref}^C \frac{Q - Q_{min}}{Q_{max} - Q_{min}}$
9)		$I_K = \frac{P_{max}^C}{\alpha^{Chl} \Theta^C}$
10)	from Eq. (1) and (2)	$\frac{dQ}{dt} = V_N^C - \mu Q$
11)	from Eq. (1) and (2)	$\frac{d\Theta^C}{dt} = V_N^C \rho_{Chl} - \Theta^C \mu$

https://doi.org/10.5194/bg-2020-314
Preprint. Discussion started: 4 September 2020

780

Table A7. Model equations of the extended model based on G98

1)	Carbon synthesis *(80% reduced C synthesis under Si limitation after Werner 1978)*	$IF\ (dSi < s_{min} * 2.3)$ $\frac{dC}{dt} = \left(P^C - \zeta V_N^C - R^C - xf\right)C = \mu C$ $ELSE$ $\frac{dC}{dt} = 0.2\left(P^C - \zeta V_N^C - R^C - xf\right)C = \mu C$
2)	Chl synthesis *(Chl synthesis stops under Si limitation after Werner 1978)*	$IF\ (dSi < s_{min} * 2.3)$ $\frac{dChl}{dt} = 0$ $ELSE$ $\frac{dChl}{dt} = \left(\frac{\rho_{Chl} V_N^C}{\Theta^C} - R_{Chl}\right) Chl$
3)	with	$\rho^{Chl} = \Theta_{max}^N \left[1 - exp\left(-\frac{I}{I_K}\right)\right]$
4)	Nitrogen uptake	$\frac{dN}{dt} = \left(\frac{V_N^C}{Q} - R^N - xf\right) N$
5)	Photosynthesis	$P^C = P_{max}^C \left[1 - exp\left(-\frac{I}{I_K}\right)\right]$

https://doi.org/10.5194/bg-2020-314
Preprint. Discussion started: 4 September 2020

6a)	Max. nitrate uptake	$V_{NO3}^{C} = V_{ref}^{C}\left[\frac{Q_{max} - Q}{Q_{max} - Q_{min}}\right]\frac{NO3}{NO3 + K_{no3}}$
6b)	Max ammonium uptake *(based on SHANIM Eq4 by Flynn and Fasham, 1997)*	$V_{NH4}^{C} = (0.01\,Q)\,0.0021\,\frac{NH4}{NH4 + K_{nh4}}$
6)	Max N uptake *(Based on Flynn and Fasham, 1997 and Flynn, 1999 showing no total inhibition in cold water)*	$IF\ (NH4 > nh4_{thresh})$ $V_N^C = V_{NH4}^C + 0.2\,V_{NO3}^C$ $ELSE$ $V_N^C = V_{NH4}^C + V_{NO3}^C$
7)	with	$V_{ref}^{C} = P_{ref}^{C} Q_{max}$
8)		$P_{max}^{C} = P_{ref}^{C}\frac{Q - Q_{min}}{Q_{max} - Q_{min}}$
9)		$I_K = \frac{P_{max}^{C}}{\alpha^{Chl}\Theta^{C}}$
10)	from Eq. (1) and (2)	$\frac{dQ}{dt} = V_N^C - \mu Q$
11)	from Eq. (1) and (2)	$\frac{d\Theta^C}{dt} = V_N^C \rho_{Chl} - \Theta^C \mu$
12)	Bacteria biomass production *(Logistic growth)*	$\frac{dBact}{dt} = Bact\ \mu_{Bact}\ (Bact_{max} - Bact)$
13)	Silicate uptake *(Monod kinetics after Spilling et al., 2009)*	$V_S^C = V_{\max}\ \ dSi\ \frac{dSi - S_{min}}{K_{si}\ S_{min}} = \frac{dpSi}{dt} = \frac{ddSi}{dt}$

https://doi.org/10.5194/bg-2020-314
Preprint. Discussion started: 4 September 2020

14)	Ammonium uptake and production *(Threshhold after Tezuka 1989)*	$IF\ (\frac{C}{N} < 10)$ $\frac{dNH4}{dt} = -\left(\frac{V_{NH4}^{C}}{Q}\right) N + Bact\ xf\ N\ rem + bact\ DON\ rem_d - \frac{Bact}{16}) / 14\ 10^3$ $ELSE$ $\frac{dNH4}{dt} = -\left(\frac{V_{NH4}^{C}}{Q}\right) N + Bact\ xf\ N\ rem - \frac{Bact}{16}) / 14\ 10^3$
15)	DON uptake and production	$IF\ (\frac{C}{N} < 10)$ $\frac{dDON}{dt} = -\frac{Bact\ xf\ N\ rem + Bact\ DON\ rem_d + xf\ N}{14\ 10^3}$ $ELSE$ $\frac{dDON}{dt} = -\frac{Bact\ xf\ N\ rem + xf\ N}{14\ 10^3}$
16)	DIN uptake	$IF\ (NH4 > nh4_{thresh})$ $\frac{dDIN}{dt} = \frac{-\left(\frac{V_{NO3}^{C}}{Q}\right) N - \frac{Bact}{16}}{14\ 10^3}$ $ELSE$ $\frac{dDIN}{dt} = \frac{-0.2\left(\frac{V_{NO3}^{C}}{Q}\right) N - \frac{Bact}{16}}{14\ 10^3}$

785

https://doi.org/10.5194/bg-2020-314
Preprint. Discussion started: 4 September 2020

Figures

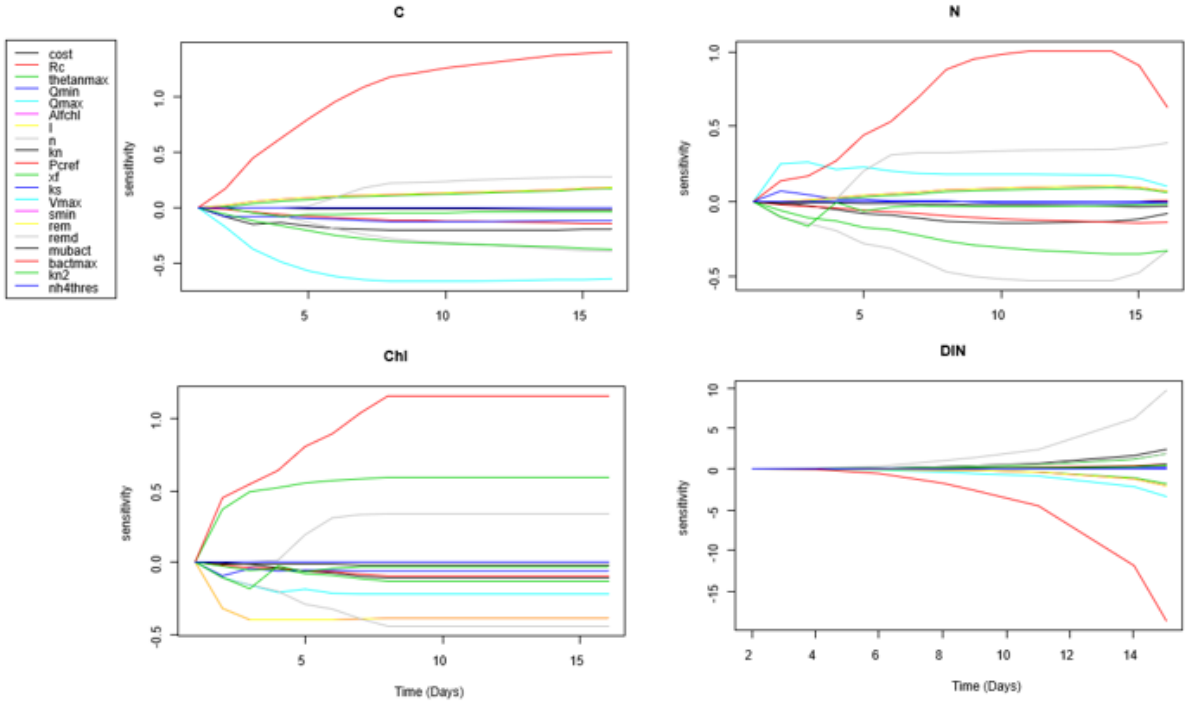

Figure B1. Sensitivity analyses of model parameters and important parameters based on the bacteria-enriched experiment. Explanation of all variable/parameters is provided in Table A2.

https://doi.org/10.5194/bg-2020-314
Preprint. Discussion started: 4 September 2020

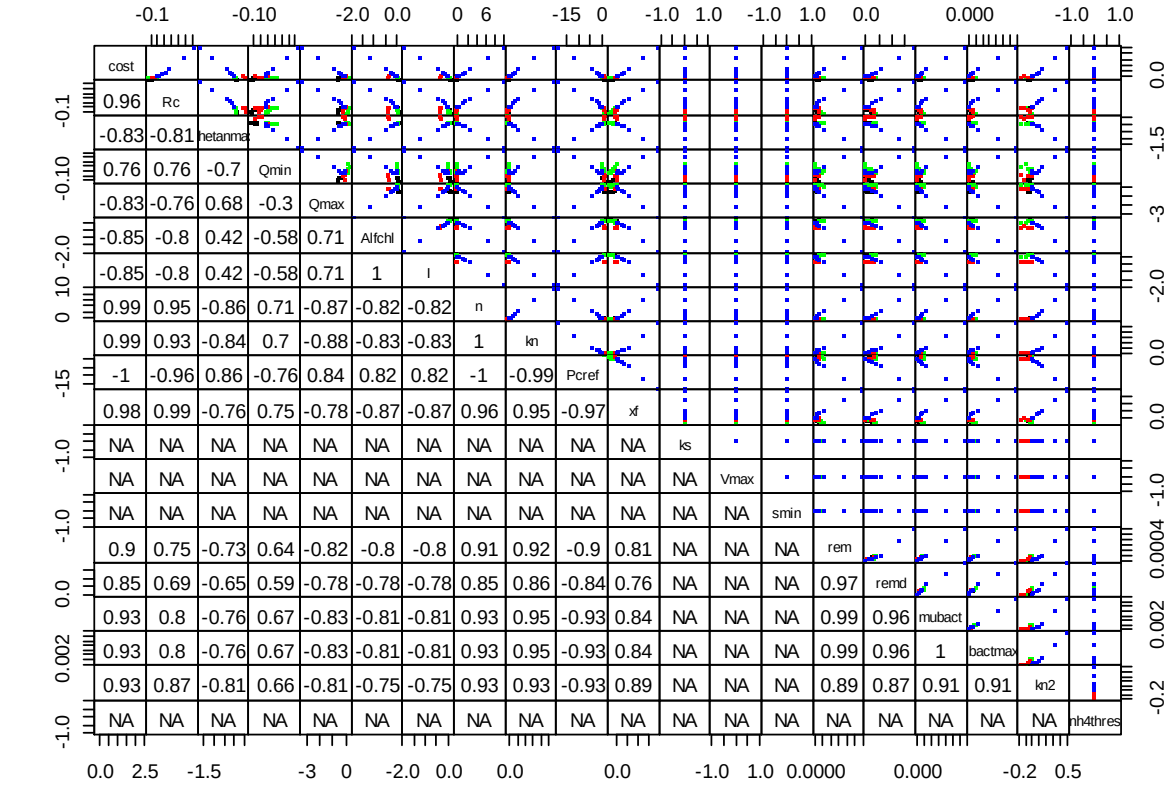

Figure B2. Collinearity analyses of the various parameters with pairs plot to the upper right and correlation coefficients to the lower left. Blue points show the response to DIN to the parameter changes, black POC, red PN, and green Chl. Explanations for the parameters are given in Table A2.

795

https://doi.org/10.5194/bg-2020-314
Preprint. Discussion started: 4 September 2020

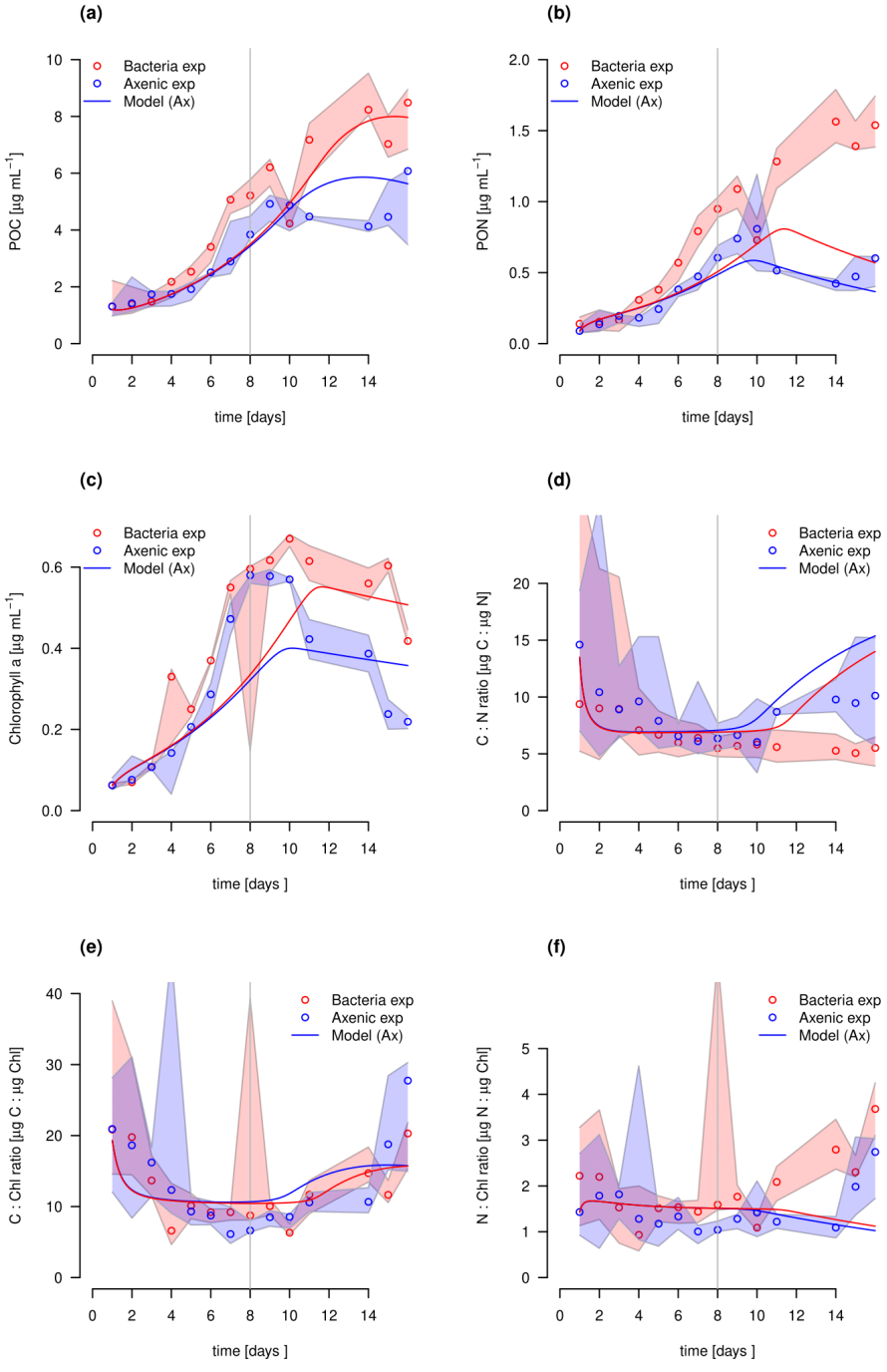

Figure B3: Model fit of the G98 model to the axenic (blue) and bacteria enriched (red) experiment. Circles show median values and the coloured polygons show the total range of measured data. Solid lines show the model outputs of a) POC, b) PON, c) Chl, d) C:N, e) C:Chl, and f) N:Chl.

https://doi.org/10.5194/bg-2020-314
Preprint. Discussion started: 4 September 2020


Biogeosciences Discussions Open Access EGU

800 **Equation**

Equation C1. normalized RMSE with i being the different variables (POC, PON, Chl, DIN), and j the different values of each state variable. Predicted values are given as P and observed values as O.

$$RMSE = \sqrt{\sum_{\substack{i=1 \\ j=1}}^{n,p} \frac{(P_{i,j} - O_{i,j})^2}{Var(O_i)}}$$

805